MPI-Ph/94-11
TUM-T31-60/94
February 1994

Direct CP Violation in $K_L \to \pi^0 e^+ e^-$ Beyond Leading Logarithms*

Andrzej J. BURAS[1,2], Markus E. LAUTENBACHER[1]
Mikołaj MISIAK[1†], Manfred MÜNZ[1]

[1] *Physik Department, Technische Universität München, D-85748 Garching, Germany.*

[2] *Max-Planck-Institut für Physik – Werner-Heisenberg-Institut, Föhringer Ring 6, D-80805 München, Germany.*

Abstract

We analyze the direct CP violation in the rare decay $K_L \to \pi^0 e^+ e^-$ with QCD effects taken into account consistently in the next-to-leading order. We calculate the two-loop mixing between the four-quark $\Delta S = 1$ operators and the operator $Q_{7V} = (\overline{s}d)_{V-A}(\overline{e}e)_V$ in the NDR and HV renormalization schemes. Using the known two-loop anomalous dimension matrix of the four-quark operators, we find that the coefficient $C_{7V}(\mu)$ depends only very weakly on μ, renormalization scheme and $\Lambda_{\overline{\rm MS}}$. The next-to-leading QCD corrections enhance the direct CP violating contribution over its leading order estimate so that it remains dominant in spite of the recent decrease of $|V_{ub}/V_{cb}|$ and $|V_{cb}|$. We expect typically $BR(K_L \to \pi^0 e^+ e^-)_{dir} \approx 6 \cdot 10^{-12}$, although values as high as 10^{-11} are not yet excluded.

*Supported by the German Bundesministerium für Forschung und Technologie under contract 06 TM 732, the CEC Science project SC1-CT91-0729 and the Polish Committee for Scientific Research.

†On leave of absence from Institute of Theoretical Physics, Warsaw University.

1 Introduction

A clear cut observation of *direct* CP violation, the violation of CP symmetry in the decay amplitudes remains as one of the central targets of high energy physics in the 90's and in the beginning of 21st century [1, 2, 3]. The CP violation in the $K \to \pi\pi$ decays discovered almost 30 years ago can be accommodated in the standard model as a result of complex phases present in K^0–$\overline{K}^0$ mixing and is usually called the *indirect* CP violation.

The Kobayashi-Maskawa description of CP violation [4] predicts also the existence of this phenomenon in the decay amplitudes with its size strongly correlated with the weak couplings of the top quark and with its mass. In this respect, a very special role is played by the ratio ϵ'/ϵ. A measurement of a non-zero $Re(\epsilon'/\epsilon)$ would automatically signal a *direct* CP violation. The experimental situation is not conclusive however. While the result of NA31 collaboration at CERN with $Re(\epsilon'/\epsilon) = (23 \pm 7) \cdot 10^{-4}$ [5] clearly indicates direct CP violation, the value of E731 at Fermilab, $Re(\epsilon'/\epsilon) = (7.4 \pm 5.9) \cdot 10^{-4}$ [6] is compatible with superweak theories in which $\epsilon'/\epsilon = 0$. Hopefully, in about five years the experimental situation concerning ϵ'/ϵ will be clarified through the improved measurements by the two collaborations at the 10^{-4} level and by experiments at the Φ factory in Frascati.

On the theoretical side a considerable progress has been made by calculating the short distance Wilson coefficients of the operators contributing to ϵ'/ϵ beyond leading logarithmic approximation [7, 8, 9, 10, 11, 12, 13, 14]. Unfortunately, there exist sizable uncertainties in the hadronic matrix elements of these operators which hopefully will be reduced when new data are available. Moreover, strong cancellations between QCD penguin and electroweak penguin contributions for large m_t make a precise theoretical prediction for $Re(\epsilon'/\epsilon)$ even harder. All efforts should be made to improve this situation.

Whereas in $K \to \pi\pi$ decays the CP violating contribution is a tiny part of the full amplitude and the direct CP violation is expected to be at least by three orders of magnitude smaller than the indirect CP violation, the corresponding hierarchies are very different for the rare decay $K_L \to \pi^0 e^+ e^-$. At lowest order in electroweak interactions (single photon, single Z-boson or double W-boson exchange), this decay takes place only if CP symmetry is violated [15, 16, 17, 18, 19]. Moreover, the direct CP violating contribution might be larger than the indirect one. The CP conserving contribution to the amplitude comes from a two photon exchange,[1] which although higher order in α could be sizable. The studies of the last years [20, 21] indicate however that the CP conserving part is significantly smaller than the direct CP violating contribution.

The size of the indirect CP violating contribution will be known once the CP conserving decay $K_S \to \pi^0 e^+ e^-$ is measured. On the other hand the direct CP violating contribution can be fully calculated as a function of m_t, CKM parameters and the QCD coupling constant α_s. There are practically no theoretical uncertainties related to hadronic matrix elements in this part, because the latter can be extracted from the well-measured decay $K^+ \to \pi^0 e^+ \nu$. In what follows, we will concentrate on this

[1] Also the QED correction to a single Z-boson or a W-box exchange can give CP conserving contributions of the same order as the two photon exchange.

contribution relegating the discussion of the other two contributions to the end of the paper.

The aim of this paper is to construct the effective Hamiltonian for $K_L \to \pi^0 e^+ e^-$,

$$H_{eff} = \frac{G_F}{\sqrt{2}} \left[\sum_{i=1}^{6} C_i(\mu) Q_i(\mu) + C_{7V}(\mu) Q_{7V}(\mu) + C_{7A}(M_W) Q_{7A}(M_W) \right] \tag{1.1}$$

with the Wilson coefficients $C_i(\mu)$ including leading and next-to-leading QCD corrections. Here $Q_{1,2}$ denote current-current operators, $Q_{3\text{–}6}$ QCD penguin operators and

$$Q_{7V} = (\bar{s}d)_{V-A}(\bar{e}e)_V, \qquad Q_{7A} = (\bar{s}d)_{V-A}(\bar{e}e)_A \tag{1.2}$$

are the operators originating in the γ- and Z^0-penguin and box diagrams of fig. 1. For simplicity the CKM parameters have been suppressed in (1.1). We will include them explicitly in section 4.1. Our paper can be considered as a generalization of the analyses [15, 16, 17, 18, 19] to include next-to-leading logarithmic QCD effects. Whereas in refs. [15, 16, 17, 18, 19] the logarithms $\alpha t(\alpha_s t)^n$ with $t = \ln(M_W^2/\mu^2)$ have been summed, the present analysis includes also the summation of the logarithms $\alpha(\alpha_s t)^n$ for which two-loop anomalous dimensions of Q_i are necessary. In this way we remove the sizeable renormalization scheme dependence of the existing leading logarithmic results. The numerical significance of such a renormalization scheme dependence has been pointed out in ref. [22].

The important observation made in refs. [17, 18, 19] is the presence of Z^0-penguin and box-diagram contributions which although small for $m_t < M_W$, compete for $m_t > M_W$ with the photonic penguins. The contributions of these new diagrams have been already included in refs. [17, 18, 19]. It should be stressed however that these additional contributions are from the point of view of the renormalization group at the next-to-leading order (NLO) and their consistent inclusion requires also the summation of next-to-leading logarithms. In view of the NLO analyses of refs. [7, 8, 9, 10, 11, 12, 13, 14], the corresponding NLO analysis for $K_L \to \pi^0 e^+ e^-$ is now substantially easier than it could have been at the time the calculations of refs. [17, 18, 19, 22] were performed.

With the complete calculation of next-to-leading contributions we will be able to study for the first time the dependence of the direct CP violation in $K_L \to \pi^0 e^+ e^-$ on the QCD scale parameter $\Lambda_{\overline{\rm MS}}$ and to remove certain ambiguities present in the analyses of refs. [17, 18, 19, 22].

Our paper is organized as follows. In section 2, we present general formulæ for $C_i(\mu)$ beyond the leading logarithmic approximation and we discuss some aspects of the renormalization scheme dependence. In section 3, we calculate the two-loop mixing between $Q_i \quad (i = 1, \ldots, 6)$ and Q_{7V}, which together with the two-loop results for Q_i of refs. [7, 8, 9, 10, 11, 12, 13, 14] gives the necessary two-loop anomalous dimension matrix for $K_L \to \pi^0 e^+ e^-$. In section 4, we present the effective Hamiltonian relevant for $K_L \to \pi^0 e^+ e^-$ and give numerical results for $C_i(\mu)$ in the NDR and HV schemes. In section 5, we calculate $BR(K_L \to \pi^0 e^+ e^-)_{dir}$ as a function of m_t and $\Lambda_{\overline{\rm MS}}$ incorporating the updated values of the CKM parameters. We also give an analytic expression for $BR(K_L \to \pi^0 e^+ e^-)_{dir}$ using the method of Penguin-Box-Expansion [23]. In section 6, we compare the contribution of the direct CP violation to $K_L \to \pi^0 e^+ e^-$ with the other two contributions. In section 7 a brief summary and outlook are given. A few technical details of the analysis have been relegated to the appendices.

2 Basic Formulæ for Wilson Coefficients

2.1 Operators

Our basis of operators is given as follows

$$\begin{aligned} Q_1 &= (\bar{s}_\alpha u_\beta)_{V-A}(\bar{u}_\beta d_\alpha)_{V-A} \\ Q_2 &= (\bar{s}u)_{V-A}(\bar{u}d)_{V-A} \\ Q_3 &= (\bar{s}d)_{V-A}\sum_q(\bar{q}q)_{V-A} \\ Q_4 &= (\bar{s}_\alpha d_\beta)_{V-A}\sum_q(\bar{q}_\beta q_\alpha)_{V-A} \\ Q_5 &= (\bar{s}d)_{V-A}\sum_q(\bar{q}q)_{V+A} \\ Q_6 &= (\bar{s}_\alpha d_\beta)_{V-A}\sum_q(\bar{q}_\beta q_\alpha)_{V+A} \\ Q'_{7V} &= (\alpha/\alpha_s)(\bar{s}d)_{V-A}(\bar{e}e)_V \\ Q_{7A} &= (\bar{s}d)_{V-A}(\bar{e}e)_A \end{aligned} \tag{2.1}$$

where α and β denote colour indices ($\alpha, \beta = 1, \ldots, N$). We omit the colour indices for the colour-singlet currents. Labels $(V \pm A)$ refer to $\gamma_\mu(1 \pm \gamma_5)$. The factor α/α_s in the definition of Q'_{7V} allows to make all the elements of the anomalous dimension matrix be of the same order in α_s. At the end of the renormalization group analysis, this factor will be put back into the Wilson coefficient $C_{7V}(\mu)$ of the operator Q_{7V} in eq. (1.2). There is no need to include a similar factor in Q_{7A} as this operator does not mix under renormalization with the remaining operators. The sums in eq. (2.1) run over the flavours active at a given scale μ.

For $\mu > m_c$ two additional current-current operators have to be taken into account

$$Q_1^c = (\bar{s}_\alpha c_\beta)_{V-A}(\bar{c}_\beta d_\alpha)_{V-A}, \qquad Q_2^c = (\bar{s}c)_{V-A}(\bar{c}d)_{V-A}. \tag{2.2}$$

It should be stressed that the form of Q_1, Q_2, Q_1^c and Q_2^c here differs from the one used by Dib, Dunietz and Gilman [17, 18] and by Flynn and Randall [19] where the corresponding Fierz conjugates have been adopted

$$\widetilde{Q}_1 = (\bar{s}d)_{V-A}(\bar{u}u)_{V-A}, \qquad \widetilde{Q}_2 = (\bar{s}_\alpha d_\beta)_{V-A}(\bar{u}_\beta u_\alpha)_{V-A}, \tag{2.3}$$

$$\widetilde{Q}_1^c = (\bar{s}d)_{V-A}(\bar{c}c)_{V-A}, \qquad \widetilde{Q}_2^c = (\bar{s}_\alpha d_\beta)_{V-A}(\bar{c}_\beta c_\alpha)_{V-A}. \tag{2.4}$$

Both bases are equally good although we somewhat prefer the basis (2.1), because Q_2 is taken in the colour singlet form as it appears in the tree level Hamiltonian. We will return later to the comparison of next-to-leading order calculations performed in these two bases.

We do not include in our analysis the electroweak four-quark penguin operators denoted as Q_7–Q_{10} in ref. [10] because their Wilson coefficients and matrix elements for $K_L \to \pi^0 e^+ e^-$ are both of order $\mathcal{O}(\alpha)$ implying that these operators enter the amplitude $A(K_L \to \pi^0 e^+ e^-)$ at $\mathcal{O}(\alpha^2)$. This should be distinguished from the case of ϵ'/ϵ. There, in spite of being suppressed by α/α_s relative to QCD penguin operators, the electroweak penguin operators have to be included in the analysis because of the

additional enhancement factor $ReA_0/ReA_2 \simeq 22$. Such an enhancement factor is not present here and the electroweak penguin operators can be safely neglected.

Concerning the Wilson coefficients, the electroweak four-quark penguin operators affect through mixing under renormalization the coefficients C_3–C_6 at $\mathcal{O}(\alpha)$ and C_{7V} at $\mathcal{O}(\alpha^2)$. Since the corresponding matrix elements are $\mathcal{O}(\alpha)$ and $\mathcal{O}(1)$ respectively, we again obtain a negligible $\mathcal{O}(\alpha^2)$ effect in $A(K_L \to \pi^0 e^+ e^-)$.

We also neglect the "magnetic moment" operators which play a crucial role in the $b \to s\gamma$ and $s \to d\gamma$ transitions. These operators, being of dimension five, do not influence the Wilson coefficients of the operators in eq. (2.1). Since their contributions to $K_L \to \pi^0 e^+ e^-$ are suppressed by an additional factor m_s, they appear strictly speaking at higher order in chiral perturbation theory.

2.2 Renormalization Group Equations

The renormalization group equation for $\vec{C}(\mu)$ is given by

$$\left[\mu\frac{\partial}{\partial\mu} + \beta(g)\frac{\partial}{\partial g}\right]\vec{C}(\frac{M_W^2}{\mu^2}, g) = \hat{\gamma}(g)\vec{C}(\frac{M_W^2}{\mu^2}, g) \tag{2.5}$$

where $\beta(g)$ is the QCD beta function

$$\beta(g) = -\beta_0\frac{g^3}{16\pi^2} - \beta_1\frac{g^5}{(16\pi^2)^2} - \ldots, \tag{2.6}$$

with

$$\beta_0 = 11 - \frac{2}{3}f, \qquad\qquad \beta_1 = 102 - \frac{38}{3}f, \tag{2.7}$$

and $f = u + d$ denoting the number of active flavours, u and d being the number of u-type and d-type flavours, respectively.

In what follows, we will neglect the running of the electromagnetic coupling constant α. This is a very good approximation because only scales $1\,\mathrm{GeV} \leq \mu \leq M_W$ are involved in our analysis. In the numerical analysis we will take $\alpha = 1/128$. For the effective QCD coupling constant we will use

$$\alpha_s^{(f)}(Q) = \frac{4\pi}{\beta_0 \ln(Q^2/\Lambda_f^2)}\left[1 - \frac{\beta_1 \ln\,\ln(Q^2/\Lambda_f^2)}{\beta_0^2 \ln(Q^2/\Lambda_f^2)}\right], \tag{2.8}$$

with Λ_f in the $\overline{MS}$ scheme. Demanding the continuity of $\alpha_s^{(f)}(Q)$ at quark thresholds in the form

$$\alpha_s^{(3)}(m_c) = \alpha_s^{(4)}(m_c), \qquad\qquad \alpha_s^{(4)}(m_b) = \alpha_s^{(5)}(m_b) \tag{2.9}$$

gives relations between the various Λ_f. In what follows we will denote $\Lambda_{\overline{\mathrm{MS}}} \equiv \Lambda_4 \equiv \Lambda_{QCD}$.

Although it has recently become popular to use $\alpha_s(M_Z)$ instead of Λ_{QCD} to parametrize the experimental knowledge about α_s, we will present our results for the Wilson coefficients as functions of Λ_4 in order to facilitate the comparison with refs. [17, 18, 19]. For each particular value of Λ_4 used, we give the corresponding value of $\alpha_s(M_Z)$ with the next-to-leading order accuracy in app. D.

Since the operator Q_{7A} does not mix with the remaining operators in eq. (2.1), we will not include its coefficient in $\vec{C}(\mu)$. Consequently, $\hat{\gamma}(g)$ in eq. (2.5) is a 7×7 anomalous dimension matrix which we expand as follows

$$\hat{\gamma}(g) = \hat{\gamma}^{(0)}\frac{g^2}{16\pi^2} + \hat{\gamma}^{(1)}\frac{g^4}{(16\pi^2)^2} + \dots \,. \tag{2.10}$$

The calculation of this matrix will be presented in section 3.

2.3 Solution for $\vec{C}(\mu)$

Following [9] we write the solution of eq. (2.5) as

$$\vec{C}(\mu) = \hat{U}(\mu, M_W)\vec{C}(M_W) \tag{2.11}$$

where the renormalization group evolution matrix is given generally by

$$\hat{U}(m_1, m_2) = T_g \exp \int_{g(m_2)}^{g(m_1)} dg' \frac{\hat{\gamma}^T(g')}{\beta(g')} \tag{2.12}$$

with $m_1 < m_2$. Here T_g denotes such ordering in the coupling constants that they increase from right to left. Expanding $\hat{\gamma}(g)$ and $\beta(g)$ as in eqs. (2.10) and (2.6) respectively one finds

$$\hat{U}(m_1, m_2) = \left(\hat{1} + \frac{\alpha_s(m_1)}{4\pi}\hat{J}\right)\hat{U}^{(0)}(m_1, m_2)\left(\hat{1} - \frac{\alpha_s(m_2)}{4\pi}\hat{J}\right) \tag{2.13}$$

where $\hat{U}^{(0)}(m_1, m_2)$ denotes the evolution matrix in the leading logarithmic approximation and $\hat{J}$ summarizes the next-to-leading corrections to this evolution. If

$$\hat{\gamma}_D^{(0)} \equiv \hat{V}^{-1}\hat{\gamma}^{(0)T}\hat{V}, \qquad\qquad \hat{G} \equiv \hat{V}^{-1}\hat{\gamma}^{(1)T}\hat{V} \tag{2.14}$$

where $\hat{\gamma}_D^{(0)}$ denotes a diagonal matrix whose diagonal elements are the components of the vector $\vec{\gamma}^{(0)}$, then

$$\hat{U}^{(0)}(m_1, m_2) = \hat{V}\left[\left(\frac{\alpha_s(m_2)}{\alpha_s(m_1)}\right)^{\vec{a}}\right]_D \hat{V}^{-1} \quad \text{with} \quad \vec{a} = \frac{\vec{\gamma}^{(0)}}{2\beta_0}. \tag{2.15}$$

For the matrix $\hat{J}$ one gets

$$\hat{J} = \hat{V}\hat{S}\hat{V}^{-1} \tag{2.16}$$

where the elements of $\hat{S}$ are given by

$$S_{ij} = \delta_{ij}\gamma_i^{(0)}\frac{\beta_1}{2\beta_0^2} - \frac{G_{ij}}{2\beta_0 + \gamma_i^{(0)} - \gamma_j^{(0)}} \tag{2.17}$$

with $\gamma_i^{(0)}$ denoting the elements of $\vec{\gamma}^{(0)}$ and G_{ij} the elements of $\hat{G}$.

2.4 The Initial Conditions $\vec{C}(M_W)$

The calculation of the initial conditions $\vec{C}(M_W)$ has been discussed at length in refs. [17, 18, 19, 12, 13]. In fact, the results for $\vec{C}(M_W)$ can be extracted from these papers. Therefore we recall here only the basic ingredients of this calculation stressing one point which has not been discussed in previous analyses of $K_L \to \pi^0 e^+ e^-$.

In order to find $\vec{C}(M_W)$, the one-loop current-current and penguin diagrams of fig. 1 with the full W and Z propagators and internal top quark exchanges have to be calculated first. Also the relevant counterterms have to be added to make the result finite. Subsequently, the result of this calculation has to be expressed in terms of matrix elements $\langle\vec{Q}(M_W)\rangle$. The latter are found by inserting the operators $\vec{Q}$ as depicted in fig. 2 into the one-loop current-current and penguin diagrams of fig. 3 and calculating the finite contributions in some renormalization scheme.

The resulting coefficients $\vec{C}(M_W)$ do not depend on the assumptions made about the properties of the external lines in figs. 1 and 3, i.e. on the infrared structure of the theory. They depend however on the renormalization scheme through the matrix elements $\langle\vec{Q}(M_W)\rangle$. In our calculation we will use as in [8, 9, 10, 11, 12, 13, 14] two renormalization schemes usually called NDR and HV.

For the NDR scheme and the basis (2.1) one finds

$$C_1(M_W) = \frac{11}{2}\frac{\alpha_s(M_W)}{4\pi}, \qquad C_2(M_W) = 1 - \frac{11}{6}\frac{\alpha_s(M_W)}{4\pi}, \tag{2.18}$$

$$C_3(M_W) = -\frac{1}{3}C_4(M_W) = C_5(M_W) = -\frac{1}{3}C_6(M_W) = -\frac{\alpha_s(M_W)}{24\pi}\widetilde{E}(x_t), \tag{2.19}$$

$$C'_{7V}(M_W) = \frac{\alpha_s(M_W)}{2\pi}\left[\frac{C(x_t) - B(x_t)}{\sin^2\theta_W} - \widetilde{D}(x_t) - 4C(x_t)\right] \tag{2.20}$$

and

$$C_{7A}(M_W) = \frac{\alpha}{2\pi}\frac{B(x_t) - C(x_t)}{\sin^2\theta_W}. \tag{2.21}$$

Here

$$\widetilde{E}(x_t) = E(x_t) - \frac{2}{3}, \qquad \widetilde{D}(x_t) = D(x_t) - \frac{4}{9}, \tag{2.22}$$

$$x_t = \frac{m_t^2}{M_W^2}\,, \tag{2.23}$$

and

$$B(x) = \frac{1}{4}\left[\frac{x}{1-x} + \frac{x\ln x}{(x-1)^2}\right], \tag{2.24}$$

$$C(x) = \frac{x}{8}\left[\frac{x-6}{x-1} + \frac{3x+2}{(x-1)^2}\ln x\right], \tag{2.25}$$

$$D(x) = \frac{-19x^3+25x^2}{36(x-1)^3} + \frac{x^2(5x^2-2x-6)}{18(x-1)^4}\ln x - \frac{4}{9}\ln x, \tag{2.26}$$

$$E(x) = \frac{x(18-11x-x^2)}{12(1-x)^3} + \frac{x^2(15-16x+4x^2)}{6(1-x)^4}\ln x - \frac{2}{3}\ln x. \tag{2.27}$$

Comparing these results with the initial conditions used in refs. [17, 18, 19] we notice some differences. In refs. [17, 18, 19] the leading order evolution matrices have been used but in the initial conditions the m_t-dependent next-to-leading terms have been already taken into account. These m_t-dependent terms represented by the functions $B(x_t)$, $C(x_t)$, $D(x_t)$ and $E(x_t)$ are renormalization scheme independent. Yet, the initial conditions may also contain scheme dependent next-to-leading terms which of course were not present in the analyses of refs. [17, 18, 19]. In the NDR scheme these scheme dependent terms enter the initial conditions for Q_1 and Q_2 and also modify the functions $E(x_t)$ and $D(x_t)$ by constant terms as given in eq. (2.22).

The additional constant terms in eq. (2.22) are absent in the case of the basis (2.3)–(2.4) used in refs. [17, 18, 19]. However, as pointed out in ref. [9, 12], in this case also the corresponding two-loop anomalous dimensions $\hat{\gamma}^{(1)}$ change so that the physical amplitudes remain independent of whether the basis (2.1) or (2.3)–(2.4) is used. This clarifies the observation made by Flynn and Randall [19] that the initial conditions for penguin operators do depend on the form of the operators. This dependence signals the necessity of going beyond the leading logarithmic approximation for $\hat{U}(m_1, m_2)$ in order to obtain physical results.

In the HV scheme the constant terms in eq. (2.22) are also absent. In addition the initial conditions $C_{1,2}(M_W)$ change. They can be found in app. A. Again, in physical quantities this change is cancelled by the corresponding change in the two-loop anomalous dimension matrix $\hat{\gamma}^{(1)}$ calculated in the HV scheme.

2.5 Renormalization Scheme Dependence of $\hat{\gamma}^{(1)}$

The renormalization scheme dependence of $\hat{\gamma}^{(1)}$ and the cancellation of scheme dependences in the final physical amplitudes have been discussed at length in refs. [8, 9, 10, 11, 12, 13, 14]. Here we would like only to recall one important relation between $(\hat{\gamma}^{(1)})_a$ and $(\hat{\gamma}^{(1)})_b$ calculated in two different renormalization schemes a and b or two different bases like (2.1) and (2.3)–(2.4). We have

$$(\hat{\gamma}^{(1)})_b = (\hat{\gamma}^{(1)})_a + \left[\Delta\hat{r}, \hat{\gamma}^{(0)}\right] + 2\beta_0\Delta\hat{r} \tag{2.28}$$

with $\Delta\hat{r} \equiv (\hat{r})_b - (\hat{r})_a$, where $(\hat{r})_i$ are defined by

$$\langle\vec{Q}(M_W)\rangle_i = \left[\hat{1} + \frac{\alpha_s(M_W)}{4\pi}(\hat{r})_i\right]\langle\vec{Q}^{(0)}\rangle. \tag{2.29}$$

Here, $\vec{Q}^{(0)}$ is a tree-level matrix element and $\langle\vec{Q}\rangle_i$ denotes renormalized one-loop matrix elements calculated in the scheme i. The matrices $(\hat{r})_i$ are obtained by calculating the finite terms in the one-loop diagrams of fig. 3.

Relation (2.28) is very useful as it allows to test compatibility of the two-loop anomalous dimension matrices calculated in two different renormalization or regularization schemes. It also plays a central role in demonstrating the scheme independence of physical quantities [9, 12]. Moreover, as demonstrated in refs. [10, 11] and in the app. C here, the relation (2.28) allows to avoid explicit calculation of two-loop diagrams involving traces $Tr(\gamma_\mu\gamma_\nu\gamma_\rho\gamma_\lambda\gamma_5)$ which are dangerous in the NDR scheme.

3 Anomalous Dimension Matrices

3.1 The Matrix $\hat{\gamma}^{(0)}$

The 6×6 submatrix of $\hat{\gamma}^{(0)}$ involving the operators Q_1–Q_6 has been calculated in ref. [15, 24, 25, 26, 27]. In our normalizations it is given in app. A of ref. [10]. Here we only give the remaining non-vanishing entries of $\hat{\gamma}^{(0)}$:

$$\gamma_{17}^{(0)} = -\frac{16}{9}N \qquad \gamma_{27}^{(0)} = -\frac{16}{9} \tag{3.1}$$

$$\gamma_{37}^{(0)} = -\frac{16}{9}N\left(u - \frac{d}{2} - \frac{1}{N}\right) \qquad \gamma_{47}^{(0)} = -\frac{16}{9}\left(u - \frac{d}{2} - N\right) \tag{3.2}$$

$$\gamma_{57}^{(0)} = -\frac{16}{9}N\left(u - \frac{d}{2}\right) \qquad \gamma_{67}^{(0)} = -\frac{16}{9}\left(u - \frac{d}{2}\right) \tag{3.3}$$

$$\gamma_{77}^{(0)} = -2\beta_0 = -\frac{22}{3}N + \frac{4}{3}f \tag{3.4}$$

where N is the number of colours. These elements have been first calculated in [16] except that $\gamma_{37}^{(0)}$ and $\gamma_{47}^{(0)}$ have been corrected in refs. [19, 28]. We agree with these final results.

3.2 The Matrix $\hat{\gamma}^{(1)}$

The 6×6 submatrix of $\hat{\gamma}^{(1)}$ involving the operators Q_1–Q_6 has been calculated in ref. [9, 14] in the NDR and HV renormalization schemes. The results presented there include also the ones obtained in refs. [7, 8] where the two-loop mixing of Q_1 and Q_2 operators has been considered. In our normalizations, the submatrix in question is given in app. B of ref. [10].

In order to calculate the remaining entries of $\hat{\gamma}^{(1)}$, one has to evaluate the two-loop penguin diagrams of fig. 4. Since these diagrams constitute a subset of the diagrams considered in [10], all the singularities necessary for the evaluation of the entries in question can be extracted for instance from tab. 2 of ref. [10]. Consequently, it was enough to change the relevant colour and electric charge factors in the diagrams of fig. 4.

Our final results for the seventh column of $\hat{\gamma}^{(1)}$ are given in the NDR scheme as follows:[2]

$$\gamma_{17}^{(1)} = \frac{8}{3}\left(1 - N^2\right), \qquad \gamma_{27}^{(1)} = \frac{200}{81}\left(N - \frac{1}{N}\right), \tag{3.5}$$

$$\gamma_{37}^{(1)} = \frac{8}{3}\left(u - \frac{d}{2}\right)\left(1 - N^2\right) + \frac{464}{81}\left(\frac{1}{N} - N\right), \tag{3.6}$$

$$\gamma_{47}^{(1)} = \left(u\frac{280}{81} + d\frac{64}{81}\right)\left(\frac{1}{N} - N\right) + \frac{8}{3}\left(N^2 - 1\right), \tag{3.7}$$

$$\gamma_{57}^{(1)} = \frac{8}{3}\left(u - \frac{d}{2}\right)\left(1 - N^2\right), \tag{3.8}$$

[2]The first six entries in the seventh row of $\hat{\gamma}^{(1)}$ vanish.

$$\gamma_{67}^{(1)} = \left(u\frac{440}{81} - d\frac{424}{81}\right)\left(N - \frac{1}{N}\right), \tag{3.9}$$

$$\gamma_{77}^{(1)} = -2\beta_1 = -\frac{68}{3}N^2 + \frac{20}{3}Nf + 4C_F f \tag{3.10}$$

where $C_F = \frac{N^2-1}{2N}$. The corresponding results for the HV scheme can either be obtained by direct calculation or by using the relation (2.28). They can be found in app. A.

As shown in app. B of the present paper, the results (3.5)–(3.10) are in agreement with those calculated independently in ref. [29], as long as the differences in the conventions used are properly taken into account. However, the present paper is the first one where the the two-loop mixing among Q_1–Q_6 from ref. [9] is consistently put together with the mixing of Q_1–Q_6 into Q_{7V}. The author of ref. [29] did not take into account that certain conventions used in ref. [9] were different from his own, and did not transform the results of ref. [9] into his own conventions (see app. B for details).

The calculation of two-loop mixings made in the NDR scheme requires some care when $Tr(\gamma_\mu\gamma_\nu\gamma_\rho\gamma_\lambda\gamma_5)$ appears in the calculation. One of the ways dealing with this problem is just to avoid appearance of such traces by making use of the fact that a Fierz rearrangement of any of the considered operators should not affect physical results. This method has been discussed at length in refs. [10, 11]. It is straightforward to extend it to the case of the operator basis containing also Q_{7V}. For the more complex cases of $\gamma_{37}^{(1)}$ and $\gamma_{47}^{(1)}$ we describe this extension in app. C. This is the method we have used to obtain the results (3.6) and (3.7).

Another method described in app. A of ref. [29] amounts to treating fermion lines with single $\{\gamma_\mu, \gamma_5\}$ as evanescent structures, i.e. structures that vanish in 4 dimensions but have to be treated as independent basic structures in D dimensions. In consequence, no algebraic inconsistencies with anticommuting γ_5 arise.[3] Getting rid of the trace $Tr(\gamma_\mu\gamma_\nu\gamma_\rho\gamma_\lambda\gamma_5)$ is achieved by introducing other evanescent structures. In the particular calculation of the two-loop mixing among the operators of the basis (2.1), the new evanescent structures can be shown to give no contribution. So the calculation in our particular case effectively amounts to anticommuting γ_5 whenever necessary (except for traces with single γ_5) and using eq. (19) of ref. [29] (or, equivalently, eq. (5.20) of ref. [10]) to get rid of the traces with γ_5.

Actually, in refs. [9, 10, 11] and in ref. [29] the two approaches were used and checked to give the same results. Also the equivalence of the physical results to the ones obtained within the HV scheme has been checked in refs. [9, 10, 11, 13, 14] for the case of mixing among the four-quark operators.

4 The Effective Hamiltonian for $K_L \to \pi^0 e^+ e^-$ Beyond Leading Logarithms

4.1 Master Formulæ for Wilson Coefficient Functions

Integrating out simultaneously W, Z and t we construct the effective Hamiltonian for $\Delta S = 1$ transitions relevant for $K_L \to \pi^0 e^+ e^-$ with the operators normalized at

[3] The triangle anomaly is also correctly reproduced.

$\mu = M_W$. Following the procedure of section 2.4 we find

$$H_{eff}(\Delta S = 1) = \frac{G_F}{\sqrt{2}} V_{ud} V_{us}^* \left\{ (1-\tau) H^{uc}(M_W) + \tau H^{ut}(M_W) \right\} \tag{4.1}$$

where

$$H^{uc}(M_W) = C_1(M_W)(Q_1 - Q_1^c) + C_2(M_W)(Q_2 - Q_2^c), \tag{4.2}$$

$$H^{ut}(M_W) = \sum_{i=1}^{6} C_i(M_W) Q_i + C'_{7V}(M_W) Q'_{7V} + C_{7A}(M_W) Q_{7A} \tag{4.3}$$

and

$$\tau = -\frac{V_{td} V_{ts}^*}{V_{ud} V_{us}^*}. \tag{4.4}$$

Here Q_i and $Q_{1,2}^c$ are the operators defined in eqs. (2.1)–(2.2) with $q = u, d, s, c, b$. Due to the GIM mechanism, there are no contributions of $Q_i (i \neq 1, 2)$ to $H^{uc}(M_W)$. The coefficients $C_i(M_W)$, $C'_{7V}(M_W)$ and $C_{7A}(M_W)$ are given in eqs. (2.18)–(2.21).

We next integrate out successively the b- and c-quarks and transform H_{eff} of eq. (4.1) from $\mu = M_W$ down to $\mu < m_c$ relevant for $K_L \to \pi^0 e^+ e^-$. This transformation can be compactly described as follows.

$$H^{uc}(M_W) \longrightarrow \sum_{i=1}^{6} z_i(\mu) Q_i + z'_{7V}(\mu) Q'_{7V}, \tag{4.5}$$

$$H^{ut}(M_W) \longrightarrow \sum_{i=1}^{6} v_i(\mu) Q_i + v'_{7V}(\mu) Q'_{7V} + C_{7A}(M_W) Q_{7A} \tag{4.6}$$

with the operators Q_i and Q'_{7V} renormalized at the scale μ. There is no renormalization of Q_{7A}. Since the charm quark has been integrated out, the penguin operators contribute also in eq. (4.5).

In writing eqs. (4.5) and (4.6) we have neglected the internal u- and c-quark contributions to the coefficient of the operator Q_{7A} because due to the vanishing of $C(x)$ and $B(x)$ as $x \ln x$ for $x \to 0$ they are very small compared to the top contribution.

The coefficients (z_i, z'_{7V}) and (v_i, v'_{7V}) are components of the seven-dimensional column vectors

$$\vec{z}(\mu) = \hat{U}_3(\mu, m_c) \vec{z}(m_c) \tag{4.7}$$

and

$$\vec{v}(\mu) = \hat{U}_3(\mu, m_c) \hat{M}(m_c) \hat{U}_4(m_c, m_b) \hat{M}(m_b) \hat{U}_5(m_b, M_W) \vec{C}(M_W) \tag{4.8}$$

with the components of $\vec{C}(M_W)$ given in eqs. (2.18)–(2.20).

The evolution matrices U_f are given by eq. (2.13) with f denoting the number of active flavours. $\hat{M}(m_i)$ is the matching matrix at quark threshold m_i. It will be discussed separately in section 4.2.

Inserting eqs. (4.5) and (4.6) into eq. (4.1) and introducing the coefficients

$$v_{7V}(\mu) = \frac{\alpha}{\alpha_s(\mu)}\, v'_{7V}(\mu), \qquad z_{7V}(\mu) = \frac{\alpha}{\alpha_s(\mu)}\, z'_{7V}(\mu) \tag{4.9}$$

we find the effective Hamiltonian relevant for the decay $K_L \to \pi^0 e^+ e^-$

$$H_{eff} = \frac{G_F}{\sqrt{2}} V_{ud} V_{us}^* \left[\sum_{i=1}^{7V} (z_i(\mu) + \tau y_i(\mu)) Q_i(\mu) + \tau y_{7A}(M_W) Q_{7A} \right] \tag{4.10}$$

where

$$y_i(\mu) = v_i(\mu) - z_i(\mu), \qquad y_{7A}(M_W) = C_{7A}(M_W). \tag{4.11}$$

In order to find $\vec{z}(\mu)$ we still need $\vec{z}(m_c)$. Due to the GIM mechanism, the coefficients $z_i(\mu)$ of the penguin operators Q_i, $i \neq 1, 2$ are zero in 5- and 4-flavour theories. The evolution in this range of μ ($\mu > m_c$) involves then only current-current operators $Q_{1,2} \equiv Q_{1,2}^u$ and $Q_{1,2}^c$ with the initial conditions

$$z_1(M_W) = C_1(M_W), \qquad z_2(M_W) = C_2(M_W) \tag{4.12}$$

where $C_{1,2}(M_W)$ are given in eq. (2.18). $Q_{1,2}^u$ and $Q_{1,2}^c$ do not mix under renormalization, and the coefficients of these two pairs of operators are equal for $\mu \geq m_c$. We then find

$$\begin{pmatrix} z_1(m_c) \\ z_2(m_c) \end{pmatrix} = \hat{U}_4(m_c, m_b) \hat{M}(m_b) \hat{U}_5(m_b, M_W) \begin{pmatrix} z_1(M_W) \\ z_2(M_W) \end{pmatrix} \tag{4.13}$$

where this time the evolution matrices $\hat{U}_{4,5}$ contain only the 2×2 anomalous dimension matrices describing the mixing between current-current operators. The matching matrix $\hat{M}(m_b)$ is in this case a 2×2 unit matrix. When the charm quark is integrated out, the operators $Q_{1,2}^c$ disappear from the effective Hamiltonian and the coefficients $z_i(\mu)$, $i \neq 1, 2$ for penguin operators become non-zero. In order to calculate $z_i(m_c)$ for penguin operators, a proper matching between effective 4- and 3-quark theories has to be made. This matching has been already discussed in detail in section 4 of ref. [12] where the first six components of $\vec{z}(m_c)$ are given. In order to find $z'_{7V}(m_c)$ which results from the diagrams of fig. 3, we simply have to rescale the result for the $z_7(m_c)$ in eq. (4.29) of ref. [12] by a factor of $-3\alpha_s/\alpha$.

In summary, the components of $\vec{z}(m_c)$ are given by eq. (4.13),

$$z_3(m_c) = -\frac{z_4(m_c)}{3} = z_5(m_c) = -\frac{z_6(m_c)}{3} = -\frac{\alpha_s(m_c)}{24\pi} F_s(m_c) \tag{4.14}$$

and

$$z'_{7V}(m_c) = -\frac{\alpha_s(m_c)}{2\pi} F_e(m_c) \tag{4.15}$$

where

$$F_s(m_c) = \begin{cases} -\frac{2}{3} z_2(m_c), & NDR \\ 0, & HV. \end{cases} \tag{4.16}$$

$$F_e(m_c) = \begin{cases} -\frac{4}{9}(3z_1(m_c) + z_2(m_c)), & NDR \\ 0, & HV. \end{cases} \tag{4.17}$$

In the NDR scheme these results are given for the basis (2.1).

4.2 The Matching Matrix $\hat{M}$

The additional matching matrix $\hat{M}$ between the operators in an f-flavour effective theory and an $(f+1)$-flavour effective theory is necessary because the QCD penguin operators have different structure in different effective theories. In our case

$$\hat{M}(m) = \hat{1} + \frac{\alpha_s(m)}{4\pi}\delta\hat{r}_s^T \tag{4.18}$$

where $\delta\hat{r}_s^T$ is a 7×7 matrix.

The procedure for finding $\hat{M}(m)$ has been outlined in ref. [12] where the 6×6 submatrix involving Q_1–Q_6 has been calculated. The remaining entries of $\delta\hat{r}_s$ can be found from the matrix $\delta\hat{r}_e$, also calculated in ref. [12], by making a simple rescaling by $-3\alpha_s/\alpha$ as in the case of $\vec{z}(m_c)$.

In summary, $\delta\hat{r}_s$ is given as follows. The non-vanishing rows in the 6×6 submatrix are given for $\mu = m_b$ and $\mu = m_c$ by

$$(\delta\hat{r}_s)_{4i} = (\delta\hat{r}_s)_{6i} = -\frac{5}{9}P_i \tag{4.19}$$

where

$$\vec{P} = (0, 0, -\frac{1}{3}, 1, -\frac{1}{3}, 1). \tag{4.20}$$

The seventh row of $\delta\hat{r}_s$ vanishes. The seventh column has the following non-vanishing elements for $\mu = m_b$:

$$(\delta\hat{r}_s)_{37} = 3(\delta\hat{r}_s)_{47} = (\delta\hat{r}_s)_{57} = 3(\delta\hat{r}_s)_{67} = -\frac{20}{9}. \tag{4.21}$$

For $\mu = m_c$, $-\frac{20}{9}$ has to be replaced by $\frac{40}{9}$.

4.3 Numerical Results for Wilson Coefficients

In tab. 1 we give numerical results for the coefficients z_i and y_i with $i = 1,\ldots,6,7V,7A$ in the NDR scheme, for $\Lambda_{\overline{\rm MS}} = 200, 300, 400\,{\rm MeV}$, $\mu = 1\,{\rm GeV}$ and $m_t = 150\,{\rm GeV}$. The results for the coefficients of Q_1–Q_6 are given for completeness. They have been analyzed in [12]. The numerical results for them presented here differ slightly from the ones in [12] because in the present paper the effect of electroweak penguins, being of higher order in α, has not been included. In tab. 2 we show the μ-dependence of z_{7V}/α for different values of $\Lambda_{\overline{\rm MS}}$ and for $m_t = 150\,{\rm GeV}$. The coefficient z_{7V} does not depend on m_t. In tab. 3 we show the μ-dependence of y_{7V}/α for different values of $\Lambda_{\overline{\rm MS}}$ and for $m_t = 150\,{\rm GeV}$. In tab. 4 we show the m_t-dependence of y_{7V}/α and y_{7A}/α for different values of $\Lambda_{\overline{\rm MS}}$ and for $\mu = 1.0\,{\rm GeV}$. Concentrating on the coefficients of Q_{7V} and Q_{7A} we observe:

- The coefficient y_{7V} is for $m_t = 150\,{\rm GeV}$ enhanced by 30–40% over the leading order result so that the suppression of this coefficient through QCD, found in [17, 18, 19], is considerably weakened. Without QCD corrections one would find

$y_{7V}/\alpha = 0.795$. For higher values of m_t the effect of next-to-leading order corrections, albeit sizeable, is weaker: 25–35% enhancement for $m_t = 200\,\text{GeV}$ and smaller for higher m_t. This feature will be clearly understood in the presentation in section 5.

- The scheme- and μ-dependences of y_{7V} are very weak as shown in particular in tab. 3. Also the dependence of y_{7V} on $\Lambda_{\overline{\text{MS}}}$ is rather weak, at most of 3% in the range of parameters considered. The weak μ-dependence is related to the fact that Q_{7V} does not carry any anomalous dimension and that for $\mu < m_c$ the coefficient y_{7V} is only influenced by QCD penguin operators because $y_1 = y_2 = 0$.

- The scheme- and μ-dependences of z_{7V} shown in tab. 2 are very strong. This implies that the calculation of the real amplitudes such as $K_S \to \pi^0 e^+ e^-$ requires the inclusion of the matrix elements of Q_1–Q_6 in order to cancel the scheme- and μ-dependences present in z_{7V}. Since the matrix elements $\langle \pi^0 e^+ e^- | Q_i | K_S \rangle$ can only be calculated using non-perturbative methods, it is clear that $K_S \to \pi^0 e^+ e^-$ and consequently the indirect CP violation in $K_L \to \pi^0 e^+ e^-$ are much harder to calculate than $BR(K_L \to \pi^0 e^+ e^-)_{dir}$.

- Inspecting tab. 4 and fig. 5 we observe in accordance with the analyses of [17, 18, 19] that at a certain value of m_t the coefficient $|y_{7A}|$ becomes larger than $|y_{7V}|$. For LO this transition takes place roughly for $m_t = 140 \pm 10\,\text{GeV}$, where the precise value depends on $\Lambda_{\overline{\text{MS}}}$. The next-to-leading order corrections shift this transition point to $m_t = 180 \pm 5\,\text{GeV}$.

5 $BR(K_L \to \pi^0 e^+ e^-)_{dir}$ Beyond Leading Logarithms

5.1 Analytic Formula

Let us introduce the numerical constant

$$\kappa = \frac{1}{V_{us}^2} \frac{\tau(K_L)}{\tau(K^+)} BR(K^+ \to \pi^0 e^+ \nu) = 4.16\,. \tag{5.1}$$

We find then as in [18]

$$BR(K_L \to \pi^0 e^+ e^-)_{dir} = \kappa (\text{Im}\lambda_t)^2 (y_{7A}^2 + y_{7V}^2) \tag{5.2}$$

where

$$\text{Im}\lambda_t = \text{Im}(V_{td} V_{ts}^*) \approx |V_{ub}|\ |V_{cb}| \sin\delta \tag{5.3}$$

in the standard parametrization of the CKM matrix.

In deriving eq. (5.2), the matrix elements of the operators Q_3–Q_6 have been neglected, i. e. we have assumed that

$$\sum_{i=3}^{6} y_i(\mu) \langle \pi^0 e^+ e^- | Q_i | K_L \rangle \ll y_{7V}(\mu) \langle \pi^0 e^+ e^- | Q_{7V} | K_L \rangle. \tag{5.4}$$

This assumption is supported by the corresponding relation for the quark-level matrix elements

$$\sum_{i=3}^{6} y_i(\mu)\langle de^+e^-|Q_i|s\rangle \ll y_{7V}(\mu)\langle de^+e^-|Q_{7V}|s\rangle \tag{5.5}$$

that can be easily verified perturbatively. The neglect of the matrix elements of the QCD penguin oerators is compatible with the very weak μ-dependence of the retained contribution.

Using next the method of the penguin-box expansion [23] we can write

$$y_{7V} = \frac{\alpha}{2\pi \sin^2\theta_W}\left(P_0 + Y(x_t) - 4\sin^2\theta_W\, Z(x_t) + P_E\, E(x_t)\right), \tag{5.6}$$

$$y_{7A} = -\frac{\alpha}{2\pi \sin^2\theta_W} Y(x_t) \tag{5.7}$$

where the gauge invariant combinations of $B(x)$, $C(x)$ and $D(x)$ are given as follows:

$$Y(x) = C(x) - B(x), \qquad Z(x) = C(x) + \frac{1}{4}D(x). \tag{5.8}$$

To a very good approximation one has for $120\,\mathrm{GeV} \le m_t \le 300\,\mathrm{GeV}$ [23]

$$Y(x_t) = 0.315 x_t^{0.78}, \qquad Z(x_t) = 0.175 x_t^{0.93}. \tag{5.9}$$

The constants P_0 and P_E summarize the contributions from scales below $\mu = M_W$. P_E is $\mathcal{O}(10^{-2})$ and consequently the last term in eq. (5.6) can be neglected. P_0 is given for different values of μ and $\Lambda_{\overline{\rm MS}}$ in tab. 5. We show there also the leading order results and the case without QCD corrections. The analytic expressions in eqs. (5.6) and (5.7) are useful as they show not only the explicit m_t-dependence, but also isolate the impact of leading and next-to-leading QCD effects. These effects modify only the constants P_0 and P_E. As anticipated from the results of section 4, P_0 is strongly enhanced relatively to the LO result. This enhancement amounts roughly to a factor of 1.6 ± 0.1. Part of this enhancement is however due to the fact that for $\Lambda_{LO} = \Lambda_{\overline{\rm MS}}$ the QCD coupling constant in the leading order is 20–30% larger than its next-to-leading order value. Calculating P_0 in LO but with the full α_s of (2.8) we have found that the enhancement amounts then to a factor of 1.33 ± 0.06. In any case the inclusion of NLO QCD effects and a meaningful use of $\Lambda_{\overline{\rm MS}}$ show that the next-to-leading order effects weaken the QCD suppression of y_{7V}. As seen in tab. 5, the suppression of P_0 by QCD corrections amounts to about 15% in the complete next-to-leading calculation.

We next find that

$$Y(x_t) - 4\sin^2\theta_W\, Z(x_t) = \begin{cases} 0.332 & \text{for} \quad m_t = 150\,\mathrm{GeV} \\ 0.431 & \text{for} \quad m_t = 200\,\mathrm{GeV} \\ 0.523 & \text{for} \quad m_t = 250\,\mathrm{GeV} \end{cases} \tag{5.10}$$

whereas in the same range of m_t the function $Y(x_t)$ changes from 0.840 to 1.863. Because of the additional constant term P_0 in eq. (5.6), the m_t-dependence of y_{7V} is rather weak and consequently the dominant m_t-dependence of $BR(K_L \to \pi^0 e^+ e^-)_{dir}$ for fixed $\mathrm{Im}\lambda_t$ originates from the coefficient of the operator Q_{7A}. In fact, for $m_t >$

$180GeV$ this operator gives larger contribution to the branching ratio than Q_{7V}. This is shown in fig. 5 where $|y_{7V}/\alpha|^2$ and $|y_{7A}/\alpha|^2$ are plotted as functions of m_t together with the leading order result and the case without QCD corrections. Finally, we note that for $m_t < 200\,\mathrm{GeV}$ the constant term proportional to P_0 constitutes at least 60% of y_{7V}.

5.2 Uncertainties Due to the Definition of m_t

At the level of accuracy at which we work we cannot address the question of the definition of m_t used here. In order to be able to analyze this question, one would have to calculate perturbative QCD corrections to the functions $Y(x_t)$ and $Z(x_t)$ and include also an additional order in the renormalization group improved perturbative calculation of P_0. The latter would require evaluation of three-loop anomalous dimension matrices, which in the near future nobody will attempt. In any case, we expect only a small correction to P_0. The uncertainty due to the choice of μ in $m_t(\mu)$ can be substantial, as stressed in refs. [30, 31, 32], and may result in 20–30% uncertainties in the branching ratios. It can only be reduced if $\mathcal{O}(\alpha_s)$ corrections to $Y(x_t)$ and $Z(x_t)$ are included. For $K^+ \to \pi^+\nu\bar{\nu}$, $K_L \to \pi^0\nu\bar{\nu}$, $B \to \mu^+\mu^-$ and $B \to X_s\nu\bar{\nu}$ this has been done in refs. [30, 31, 32]. The inclusion of these corrections reduces the uncertainty in the corresponding branching ratios to a few percent. Fortunately, the result for the corrected function $Y(x_t)$ given in refs. [30, 31, 32] can be directly used here. The message of refs. [30, 31, 32] is the following: For $m_t = \overline{m}_t(m_t)$, the QCD corrections to $Y(x_t)$ are below 2%. Corresponding corrections to $Z(x)$ are not known. Fortunately, the m_t-dependence of y_{7V} is much weaker and the uncertainty due to the choice of μ in $m_t(\mu)$ is small. On the basis of these arguments and the result of refs. [30, 31, 32] we believe that if $m_t = \overline{m}_t(m_t)$ is chosen, the additional QCD corrections to $BR(K_L \to \pi^0 e^+ e^-)_{dir}$ should be small.

5.3 Numerical Analysis

In the numerical calculation we need the value of $\mathrm{Im}\lambda_t$ which can be extracted from the usual analysis of the parameter ϵ that measures indirect CP violation. The formula for ϵ can be found for instance in section 7 of ref. [12] as well as in many other papers and will not be repeated here. We only give the values of the parameters which we use here. We take $|V_{us}| = 0.22$,

$$\eta_1 = 1.1[33], \quad \eta_2 = 0.57[34], \quad \eta_3 = 0.36[35,\ 36,\ 37,\ 38] \text{ (leading order)}. \tag{5.11}$$

and

$$\text{Range a: } |V_{cb}| = 0.040 \pm 0.005,\ |V_{ub}/V_{cb}| = 0.08 \pm 0.02,\ B_K = 0.70 \pm 0.20, \tag{5.12}$$

The analysis of ϵ gives two solutions for the CKM phase δ. The values of $\mathrm{Im}\lambda_t$ decrease with increasing m_t and this decrease is stronger for δ in the second quadrant. The dependence of $\mathrm{Im}\lambda_t$ on m_t compensates the corresponding m_t-dependence of y_{7V} and y_{7A}. As a result, $BR(K_L \to \pi^0 e^+ e^-)_{dir}$ decreases with m_t for the solution II and is increasing with m_t for the solution I substantially slower than one would expect

from eq. (5.2) would $\mathrm{Im}\lambda_t$ be independent of m_t. In tab. 6 we show the values of $BR(K_L \to \pi^0 e^+ e^-)_{dir}$ in units of 10^{-12} for $B_K = 0.7$, $|V_{cb}| = 0.041$, $|V_{ub}/V_{cb}| = 0.10$ as a function of m_t. For $m_t \leq 140\,\mathrm{GeV}$, ϵ cannot be fitted for these choice of parameters. In fig. 6 we present the results when the parameters are varied in the full range given in (5.12). In order to illustrate the impact of possible future improvements in the determination of B_K and the CKM parameters, in figs. 7 and 8 we show the results when smaller ranges of parameters given by

$$\text{Range b: } |V_{cb}| = 0.040 \pm 0.002,\ |V_{ub}/V_{cb}| = 0.08 \pm 0.01,\ B_K = 0.75 \pm 0.05 \tag{5.13}$$

$$\text{Range c: } |V_{cb}| = 0.043 \pm 0.002,\ |V_{ub}/V_{cb}| = 0.09 \pm 0.01,\ B_K = 0.55 \pm 0.05 \tag{5.14}$$

are used. B_K in range b is in the ball park of most recent lattice ($B_K = 0.825 \pm 0.027 \pm 0.023$) [39] and $1/N$ ($B_K = 0.7 \pm 0.1$) [40] results. In range c it is closer to the values obtained in the hadron duality approach ($B_K = 0.4 \pm 0.1$) [41]. In the latter case we had to take larger values for $|V_{cb}|$ in order to obtain solutions in the ϵ-analysis.

Finally in fig. 9 we show the ratio $BR(K_L \to \pi^0 e^+ e^-)/(\mathrm{Im}\lambda_t)^2$ as a function of m_t. All these results are self explanatory and we only make a few comments:

- The NLO corrections enhance the direct CP violating contributions with respect to its LO estimate.

- Due to large uncertainties in $\mathrm{Im}\lambda_t$ which enters the branching ratio quadratically, the enhancement found here cannot be appreciated yet. However as seen in figs. 7 and 8 the more accurate data for $\mathrm{Im}\lambda_t$ in the future will allow to feel this enhancement clearly.

- For central values of the parameters in range a and $m_t = 170 \pm 30\,\mathrm{GeV}$ we find

$$BR(K_L \to \pi^0 e^+ e^-)_{dir} = \begin{cases} (4.9 \pm 0.5) \cdot 10^{-12}, & \text{Solution I} \\ (3.7 \pm 0.5) \cdot 10^{-12}, & \text{Solution II,} \end{cases} \tag{5.15}$$

  but as seen in fig. 6 values as high as 10^{-11} are not excluded when the solution I is chosen.

The analysis of B^0–$\bar{B}^0$ mixing can constrain further the predicted values of $BR(K_L \to \pi^0 e^+ e^-\ )_{dir}$. The usual box diagrams with top quark exchanges give for the mixing parameter

$$x_d = 3.89 \cdot 10^3 \left[\frac{\tau_B}{1.5\,\mathrm{ps}}\right] \left[\frac{B_B F_B^2}{(200\,\mathrm{MeV})^2}\right] |V_{td}|^2 S(x_t), \tag{5.16}$$

where

$$S(x) = \frac{x}{4}\left(1 + \frac{9}{1-x} - \frac{6}{(1-x)^2}\right) + \frac{3x^3}{2(x-1)^3} \ln x. \tag{5.17}$$

We use

$$\sqrt{B_B}\, F_B = 200 \pm 30\,\mathrm{MeV} \tag{5.18}$$

which is in the ball park of various lattice and QCD sum rule estimates [42]. Setting $\tau_B = 1.5\,\mathrm{ps}$ we require

$$x_d = 0.72 \pm 0.08\,[43] \tag{5.19}$$

in accordance with the most recent average of CLEO and ARGUS data. The impact of B^0–$\overline{B}^0$ mixing with $\sqrt{B_B}F_B$ as given above is shown in figs. 6–8 for the NLO results as a solid line within the dark shaded area. With this additional requirement the region to the right of the solid line is excluded. The constraint is invisible for solution I. For solution II we observe that for higher values of m_t the constraint coming from B^0–$\overline{B}^0$ mixing is rather effective. These features are in accordance with general expectations that for high values of m_t and F_B the solution I is favoured and that with more precise high values of F_B the solution II could even be excluded. This would also constrain the values for $BR(K_L \to \pi^0 e^+ e^-\ )_{dir}$ for solution I.

6 Comparison with the Other Two Contributions

Now we want to compare the results obtained in the previous section with the estimates made for the indirect CP-violating contribution and the CP-conserving one. The most recent summary of the present status has been given by Pich [21]. We have nothing to add to this issue here and only state his final conclusions.

The indirect CP violating contribution is given by the $K_S \to \pi^0 e^+ e^-$ amplitude times the CP parameter ϵ. Once $BR(K_S \to \pi^0 e^+ e^-)$ has been accurately measured, it will be possible to calculate this contribution precisely. Using chiral perturbation theory it is however possible to get an estimate by relating $K_S \to \pi^0 e^+ e^-$ to the $K^+ \to \pi^+ e^+ e^-$ transition. Present data implies

$$BR(K_L \to \pi^0 e^+ e^-)_{indir} \leq 1.6 \cdot 10^{-12}, \tag{6.1}$$

i. e. a branching ratio more than a factor of 2 below the direct CP violating contribution for the CKM phase δ in the second quadrant. More importantly, if the solution I is chosen, the direct CP violating contribution is by a factor of 5 or more larger than the indirect one. This should be contrasted with $K \to \pi\pi$ decays. It should be stressed, however, that in reality the CP indirect amplitude may interfere with the vector part of the CP direct amplitude [4]. This interference could have both signs. For a very heavy top quark for which the first quadrant is favoured and the axial-vector contribution to the direct CP violation dominates, the presence of the indirect CP violation will not have a large impact on our analysis given above. Yet for $m_t = \mathcal{O}(150\,\mathrm{GeV})$ and δ in the second quadrant, the indirect CP violation cannot be neglected and a more careful estimate of the full CP violating branching ratio requires a better analysis which includes the interference in question.

The estimate of the CP conserving contribution is more difficult. We refer the reader to ref. [21] where the literature on this subject can be found. The most recent analysis in the framework of chiral perturbation theory gives [20]

$$BR(K_L \to \pi^0 e^+ e^-)_{cons} \approx (0.3 - 1.8) \cdot 10^{-12}, \tag{6.2}$$

i. e. well below the *direct* CP violating contribution. An improved estimate of this component of $K_L \to \pi^0 e^+ e^-$ is certainly desirable.

[4] The axial part of the CP indirect amplitude can be safely neglected

7 Summary and Outlook

We have calculated the direct CP violating contribution to $K_L \to \pi^0 e^+ e^-$ beyond the leading logarithmic approximation. This required the evaluation of two-loop mixing between the four-quark operators Q_1–Q_6 and the semileptonic operator Q_{7V}. Our main findings can be summarized as follows:

- The next-to-leading QCD corrections enhance the branching ratio $BR(K_L \to \pi^0 e^+ e^-)_{dir}$ so that its suppression found in the leading order analysis is considerably weakened.

- The net QCD suppression of this contribution for $m_t > 150\,\mathrm{GeV}$ is at most 20%.

- The very weak dependences of the resulting $BR(K_L \to \pi^0 e^+ e^-)_{dir}$ on $\Lambda_{\overline{\rm MS}}$ and μ indicate that this branching ratio can be reliably calculated in the Standard Model, provided m_t and the CKM parameters have been better determined.

- With the help of the two-loop calculation of refs. [30, 31, 32] we have also some control over the renormalization scale of m_t. Consequently when $m_t = \overline{m}_t(m_t)$ is chosen we expect on the basis of refs. [30, 31, 32] that still higher order QCD corrections are very small.

- Provided the phase δ is in the first quadrant and $m_t = 170 \pm 30\,\mathrm{GeV}$ we expect

$$BR(K_L \to \pi^0 e^+ e^-)_{dir} = \begin{cases} (6.0 \pm 4.0) \cdot 10^{-12}, & \text{Range a} \\ (4.5 \pm 1.5) \cdot 10^{-12}, & \text{Range b} \\ (7.5 \pm 2.5) \cdot 10^{-12}, & \text{Range c} \end{cases} \tag{7.1}$$

  for the three ranges of parameters considered. As seen from (7.1) the present prediction, range a, will be improved when the CKM parameters and B_K have been better determined and the top quark has been discovered. For δ in the second quadrant the branching ratio is typically by a factor of two smaller.

- These results confirm the expectations made previously by other authors that the decay $K_L \to \pi^0 e^+ e^-$ is dominated by direct CP violation (see [21] and references therein). The present experimental bounds

$$BR(K_L \to \pi^0 e^+ e^-) \le \begin{cases} 4.3 \cdot 10^{-9} & [44] \\ 5.5 \cdot 10^{-9} & [45] \end{cases} \tag{7.2}$$

  are still by three orders of magnitude away from the theoretical expectations in the Standard Model. Yet the prospects of getting the required sensitivity of order 10^{-11}–10^{-12} in five years are encouraging [1, 2, 3].

Acknowledgment

M. Misiak would like to thank A. Pich for helpful discussions.

Appendices

A Calculation in the HV Scheme

The Wilson coefficients in the HV scheme can be found using

$$\vec{C}_{HV}(\mu) = \left[\hat{\mathbf{1}} - \frac{\alpha_s(\mu)}{4\pi}\Delta\hat{r}^T\right]\vec{C}_{NDR}(\mu), \tag{A.1}$$

where $\Delta\hat{r}$ has been defined in (2.29). The 6×6 submatrix of $\Delta\hat{r}$ relating HV and NDR schemes is given in eqs. (3.9)–(3.13) of ref. [9]. Performing an analogous calculation in the presence of Q'_{7V} one finds the additional non-vanishing elements of $\Delta\hat{r}$:

$$(\Delta\hat{r})_{17} = -(\Delta\hat{r})_{47} = \frac{8}{9}N, \quad (\Delta\hat{r})_{27} = -(\Delta\hat{r})_{37} = \frac{8}{9}, \quad (\Delta\hat{r})_{77} = 2C_F. \tag{A.2}$$

The last result can be traced back to the non-vanishing anomalous dimension γ_J of the weak current at the two-loop level in the HV scheme. Consequently in this scheme the operators Q_{7V} and Q_{7A} carry anomalous dimensions at the two-loop level. Similarly the anomalous dimensions of the operators Q_1–Q_6 receive additional large contributions which are related to $\gamma_J \neq 0$ in the HV scheme. This feature introduces an unnecessarily large scheme dependence at the lower end of the renormalization group evolution. In the spirit of [12] we perform therefore an additional finite renormalization which removes these additional contributions to the anomalous dimensions of Q_1–Q_6 and makes the anomalous dimensions of Q_{7V} and Q_{7A} in the HV scheme to be zero. This transformation is equivalent to the following changes in $\Delta\hat{r}$ of (A.2):

$$(\Delta\hat{r})_{6\times 6} \;\to\; (\Delta\hat{r})_{6\times 6} - 4C_F\hat{\mathbf{1}}_{6\times 6}, \tag{A.3}$$

$$(\Delta\hat{r})_{77} \;\to\; (\Delta\hat{r})_{77} - 2C_F = 0. \tag{A.4}$$

The shift in the element (7,7) differs from the shift in (A.3). Therefore, according to eq. (2.28) this finite renormalization modifies also the mixing of the operators Q_1–Q_6 with Q'_{7V}. Using (2.28), the matrix $\hat{\gamma}^{(1)}$ calculated in the NDR scheme and $\Delta\hat{r}$ discussed above we find $\hat{\gamma}^{(1)}$ in the HV scheme modified by the finite transformations (A.3) and (A.4). Here we give only the seventh column of $\hat{\gamma}^{(1)}_{HV}$:

$$\left(\gamma^{(1)}_{17}\right)_{HV} = \frac{8}{3}\left(1-N^2\right), \qquad \left(\gamma^{(1)}_{27}\right)_{HV} = \frac{520}{81}\left(\frac{1}{N}-N\right), \tag{A.5}$$

$$\left(\gamma^{(1)}_{37}\right)_{HV} = \frac{8}{3}\left(u-\frac{d}{2}\right)\left(1-N^2\right) + \frac{256}{81}\left(N-\frac{1}{N}\right), \tag{A.6}$$

$$\left(\gamma^{(1)}_{47}\right)_{HV} = \left(\frac{520}{81}u - \frac{128}{81}d\right)\left(\frac{1}{N}-N\right) + \frac{8}{3}\left(N^2-1\right), \tag{A.7}$$

$$\left(\gamma^{(1)}_{57}\right)_{HV} = \frac{8}{3}\left(u-\frac{d}{2}\right)\left(1-N^2\right), \tag{A.8}$$

$$\left(\gamma^{(1)}_{67}\right)_{HV} = \left(\frac{376}{81}u - \frac{56}{81}d\right)\left(\frac{1}{N}-N\right), \tag{A.9}$$

$$\left(\gamma^{(1)}_{77}\right)_{HV} = -2\beta_1. \tag{A.10}$$

We observe that $\gamma_{17}^{(1)}$, $\gamma_{57}^{(1)}$ and $\gamma_{77}^{(1)}$ are the same in both schemes.

Finally we give the initial conditions in the HV scheme:

$$C_1(M_W) = \frac{7}{2}\frac{\alpha_s(M_W)}{4\pi}, \qquad\qquad C_2(M_W) = 1 - \frac{7}{6}\frac{\alpha_s(M_W)}{4\pi}. \tag{A.11}$$

The other coefficients are given in eqs. (2.19)–(2.24) with the constant pieces in (2.22) removed.

B Evanescent Differences

As described in section 3.2, the two-loop anomalous dimension matrix entries $\gamma_{17}^{(1)} - \gamma_{67}^{(1)}$ in eqs. (3.5)–(3.9) have been extracted from the calculations presented in refs. [9, 10, 11]. In this appendix, we would like to show that all the $\gamma_{17}^{(1)} - \gamma_{67}^{(1)}$ found here agree with the mixings found independently by one of us in ref. [29], after the differences in the conventions used are taken into account.

The operators responsible for the $b \to s e^+ e^-$ decay considered in ref. [29] differ from the ones in eq. (2.1) of the present paper only by changes in flavours and by trivial normalization factors. The changes in flavours are irrelevant for the values of the mixings, as long as the numbers of active up- and down-quarks are kept as free variables, which was the case in both papers. In the present paper, we have followed the normalization conventions of refs. [8, 9, 10, 11]. In consequence, the operators Q_1–Q_6 in eq. (2.1) here are four times larger than O_1 – O_6 in eq. (3) of ref. [29]. The operator Q'_{7V} here is two times larger than O_9 defined in eqs. (3) and (6) of ref. [29]. Comparing in addition eqs. (2.10) here and (20) in ref. [29] one verifies that

$$\begin{array}{rcll} \gamma_{i7}^{(0)} & = & 4B_{i3}^1, & i = 1, \ldots, 6, \\ \gamma_{i7}^{(1)} & = & 4\left(B_{i3}^2 + \Delta B_{i3}^2\right), & i = 1, \ldots, 6 \end{array} \tag{B.1}$$

where the quantities on the l.h.s are the ones from eqs. (3.1)–(3.3) and (3.5)–(3.9) of the present paper, while B_{i3}^1 and B_{i3}^2 are taken from eq. (21) of ref. [29] with the following substitutions made:

$$\overline{Q} = uQ_u + dQ_d = \frac{2}{3}\left(u - \frac{d}{2}\right), \qquad\qquad f = u + d \qquad \text{and} \qquad \xi = 0. \tag{B.2}$$

Finally, ΔB_{i3}^2 is the shift required in order to take into account the difference between the renormalization schemes used. In the following, we will check that its value is exactly what is required for eq. (B.1) to hold.

In the present calculation we have used the results of refs. [9, 10, 11] obtained within the $\overline{MS}$ scheme and NDR regularization. This was also the scheme used in ref. [29]. However, in order to fully specify a scheme, one also has to fix certain convention-dependent constants in the definitions of the evanescent operators, whenever such operators enter the game. Generalizing eq. (15) of ref. [29], one can write the evanescent operators relevant in our calculation in the following form:

$$O_{i+10}^{ev} \equiv \frac{1}{6} O_i \left(\gamma_\mu \to \gamma_{[\mu}\gamma_\nu\gamma_{\rho]}\right) \pm [1 + b_i(4 - D)]O_i, \qquad i = 1, \ldots, 6 \tag{B.3}$$

with "−" for $i = 1, \ldots, 4$ and "+" for $i = 5, 6$. D denotes the dimensionality of spacetime. The numbers b_i are arbitrary. Each choice of them corresponds to a different renormalization scheme.

In ref. [29] all the b_i's were set to zero. On the other hand, in the papers [8, 9, 10, 11] they differed from zero, and they were fixed by requiring that certain projections of the evanescent operators vanish. For $i = 1, \ldots, 4$, the relevant identity was (see eq. (4.3) of ref. [10])[5]

$$\begin{aligned} 0 = E_{\alpha\beta,\gamma\delta}\left(\gamma_\tau(1+\gamma_5)\right)_{\beta\gamma}\left(\gamma^\tau(1+\gamma_5)\right)_{\delta\alpha} &= 2Tr\{\tfrac{1}{6}\gamma_{[\mu}\gamma_\nu\gamma_{\rho]}\gamma_\tau\gamma^{[\mu}\gamma^\nu\gamma^{\rho]}\gamma^\tau(1+\gamma_5) - \\ -[1+b_i(4-D)]\gamma_\mu\gamma_\tau\gamma^\mu\gamma^\tau(1+\gamma_5)\} &= 64(4-D)(b_i-\tfrac{1}{6}). \end{aligned} \tag{B.4}$$

Eq. (4.8) of ref. [10] gives the corresponding requirement for $i = 5, 6$:

$$\begin{aligned} 0 = E_{\alpha\beta,\gamma\delta}(1-\gamma_5)_{\beta\gamma}(1+\gamma_5)_{\delta\alpha} &= 2Tr\{\tfrac{1}{6}\gamma_{[\mu}\gamma_\nu\gamma_{\rho]}\gamma^{[\mu}\gamma^\nu\gamma^{\rho]}(1+\gamma_5) + \\ +[1+b_i(4-D)]\gamma_\mu\gamma^\mu(1+\gamma_5)\} &= 32(4-D)(b_i+\tfrac{5}{6}). \end{aligned} \tag{B.5}$$

Consequently, the conventions of refs. [8, 9, 10, 11] correspond to taking

$$b_1 = b_2 = b_3 = b_4 = \frac{1}{6}, \qquad\qquad b_5 = b_6 = -\frac{5}{6}. \tag{B.6}$$

In the following, we will use the notation of ref. [29] to find the explicit values of ΔB^2_{i3} for $i = 1, \ldots, 6$.

According to eq. (16) of ref [29], the contribution of the evanescent operators to the two-loop anomalous dimension matrix for the "usual" operators depends on the divergences they renormalize (matrix a^{11}_{ik}) and on their finite one-loop matrix elements (matrix a^{01}_{kj}). The matrix a^{11}_{ik} is insensitive to the $\mathcal{O}(4-D)$ parts of the evanescent operators, i.e. it is insensitive to shifts in the numbers b_i. However, the finite one-loop matrix elements of the evanescent operators depend on these numbers. If one changes b_i from zero to any nonzero value, then the corresponding change in the one-loop matrix element of O^{ev}_{i+10} is proportional to the product of b_i and the divergent part of the one-loop matrix element of the "normal" operator that is multiplied by b_i in the definition of O^{ev}_{i+10}. Explicitly:

$$\Delta a^{01}_{(i+10)j} = a^{11}_{ij}(\pm b_i). \tag{B.7}$$

Consequently, according to eqs. (8), (16), (20) and (21) of ref. [29], one gets

$$\Delta B^2_{i3} = 16\pi^2 \sum_{k=1}^{6} a^{11}_{i(k+10)} B^1_{k3}(\pm b_k), \qquad i = 1, \ldots, 6 \tag{B.8}$$

with "−" for $i = 1, \ldots, 4$ and "+" for $i = 5, 6$. Taking the numbers b_i from eq. (B.6) above, and the matrices a^{11} and B^1 from eqs. (17) and (21) of ref. [29], respectively, one obtains the final result for ΔB^2_{i3}

$$\Delta B^2_{i3} = \left[\frac{2}{3}Nc_FQ_u,\ \ \frac{4}{3}c_FQ_u,\ \ \frac{8}{3}c_FQ_d,\ \ \frac{4}{3}c_F\overline{Q} + \frac{4}{3}Nc_FQ_d,\ \ 0,\ \ \frac{20}{3}c_F\overline{Q}\right]_i \tag{B.9}$$

[5] We neglect irrelevant terms of order $\mathcal{O}((4-D)^2)$ in eqs. (B.3), (B.4) and (B.5) here.

which is exactly what is needed for eq. (B.1) to hold.

We have thus shown that the mixings of the four-quark operators into the quark-lepton operator found in ref. [29] are in agreement with the ones found here on the basis of the results of refs. [9, 10, 11], as long as the differences in the conventions are properly taken into account. This suggests that the disagreement between refs. [29] and [46] (see app. B of ref. [29]) should be resolved in favour of ref. [29]. However, we have to point out that the next-to-leading matching conditions and mixings of the four-quark operators from ref. [9] have not been used in a fully consistent manner in ref. [29]. As long as one wants to define the evanescent operators as in ref. [29] (all the numbers b_i vanishing), one has to transform accordingly both the next-to-leading terms in the matching conditions for the the four-quark operators Q_1 and Q_2, and the whole 6×6 next-to-leading anomalous dimension matrix of the four-quark operators that has been calculated in ref. [9]. The author of ref. [29] was not aware of the fact that the conventions used in ref. [9] for the evanescent operators were different from his own. In consequence, the numerical results of ref. [29] for the $b \to s\, e^+\, e^-$ decay are somewhat larger than they should be. The change is however phenomenologically irrelevant since it never exceeds 3% .

C Calculation of $\gamma_{37}^{(1)}$ and $\gamma_{47}^{(1)}$ in the NDR Scheme

The procedure described below constitutes a synthesis of subsection 5.1 of refs. [10, 11]. The calculation is more complicated than in the pure QCD case of ref. [10] because here we only deal with pure $\mathcal{O}(\alpha_s^2)$ anomalous dimension matrices after a proper rescaling of Q_{7V}.

In order to solve the problem of closed fermion loops involving γ_5 in the NDR scheme, we have to consider four different bases of operators. All four bases contain the penguin operators Q_3 – Q'_{7V} of eq. (2.1) but differ in the current–current operators Q_1 and Q_2. The latter are given as follows,

$$\textbf{Basis A:}\ Q_1^{(u)} = (\bar{s}_\alpha u_\beta)_{V-A}\,(\bar{u}_\beta d_\alpha)_{V-A}\ , \quad Q_2^{(u)} = (\bar{s}u)_{V-A}\,(\bar{u}d)_{V-A}\ . \tag{C.1}$$

$$\textbf{Basis B:}\ Q_1^{(d)} = (\bar{s}_\alpha d_\beta)_{V-A}\left(\bar{d}_\beta d_\alpha\right)_{V-A}\ , \quad Q_2^{(d)} = (\bar{s}d)_{V-A}\left(\bar{d}d\right)_{V-A}\ . \tag{C.2}$$

$$\textbf{Basis C:}\ \widetilde{Q}_1^{(u)} = (\bar{s}d)_{V-A}\,(\bar{u}u)_{V-A}\ , \quad \widetilde{Q}_2^{(u)} = (\bar{s}_\alpha d_\beta)_{V-A}\,(\bar{u}_\beta u_\alpha)_{V-A}\ . \tag{C.3}$$

$$\textbf{Basis D:}\ \widetilde{Q}_1^{(d)} = (\bar{s}d)_{V-A}\left(\bar{d}d\right)_{V-A}\ , \quad \widetilde{Q}_2^{(d)} = (\bar{s}_\alpha d_\beta)_{V-A}\left(\bar{d}_\beta d_\alpha\right)_{V-A}\ . \tag{C.4}$$

The basis A is the standard basis of eq. (2.1) and the basis B is an auxiliary basis needed for the solution of the problem. The bases C and D are simply Fierz conjugates of Q_1 and Q_2 in A and B, respectively. Evidently,

$$Q_1^{(d)} \;=\; \widetilde{Q}_2^{(d)}\,, \qquad Q_2^{(d)} \;=\; \widetilde{Q}_1^{(d)}\,. \tag{C.5}$$

Let us next denote by $[Q_i]_1$ and $[Q_i]_2$ the result of the type-1 (closed fermion loop) and type-2 insertions (no closed fermion loop) of an operator Q_i, respectively. Then

the results for penguin contributions to the row entries of $\gamma^{(1)}$ for Q_3 and Q_4 can be written as follows

$$[Q_3]_{\rm p} = u\,[\widetilde{Q}_1^{(u)}]_1 + d\,[\widetilde{Q}_1^{(d)}]_1 + 2\,[\widetilde{Q}_1^{(d)}]_2\,, \tag{C.6}$$

$$[Q_4]_{\rm p} = u\,[\widetilde{Q}_2^{(u)}]_1 + d\,[\widetilde{Q}_2^{(d)}]_1 + 2\,[\widetilde{Q}_2^{(d)}]_2\,. \tag{C.7}$$

For the calculation of the entries in the first six columns it is not necessary to introduce the bases B and D because in pure QCD no distinction is made between $Q_{1,2}^{(u)}$ and $Q_{1,2}^{(d)}$. This was in fact the case considered in ref. [10]. However, here the seventh column involves couplings to the photon and as in ref. [11] the bases B and D have to be introduced.

There are six independent entries in eq. (C.6) and eq. (C.7) which have to be found. In the following four steps the quoted results for these entries are given for the seventh column only.

Step 1:
$[\widetilde{Q}_1^{(d)}]_2$ and $[\widetilde{Q}_2^{(d)}]_2$ can be calculated without any problems by evaluating the diagrams of fig. 4. The contributions to the seventh column are given by

$$[\widetilde{Q}_1^{(d)}]_2 = -\frac{464}{81}\,C_F\,, \tag{C.8}$$

$$[\widetilde{Q}_2^{(d)}]_2 = -\frac{1}{2}\,[Q_1^{(u)}]_2 = \frac{8}{3}\,N\,C_F\,. \tag{C.9}$$

Step 2:
$\widetilde{Q}_1^{(u)}$ and $\widetilde{Q}_2^{(u)}$ receive contributions only from type-1 insertions. This allows to find $[\widetilde{Q}_1^{(u)}]_1$ and $[\widetilde{Q}_2^{(u)}]_1$ by comparing the two–loop anomalous dimension matrices calculated in the bases C and A using the relation

$$(\hat{\gamma}^{(1)})_p^{(C)} = (\hat{\gamma}^{(1)})_p^{(A)} + \left[\Delta\hat{r}, \hat{\gamma}^{(0)}\right] + 2\,\beta_0\,\Delta\hat{r}\,, \tag{C.10}$$

where

$$\Delta\hat{r} = [\hat{r}]_C - [\hat{r}]_A \tag{C.11}$$

with $\hat{r}$ defined in eq. (2.29).

Because the insertion in the current-current diagrams are identical for these two bases, only penguin diagram contributions to $\hat{\gamma}^{(1)}$ and $\Delta\hat{r}$ enter this relation. On the other hand $\hat{\gamma}^{(0)}$ is the full one-loop matrix discussed in section 3.1. A simple calculation of finite terms in one-loop penguin diagrams gives

$$\Delta\hat{r} = -\frac{1}{3}\begin{pmatrix} 0 \\ 1 \\ 0 \\ \vdots \\ 0 \end{pmatrix} P + \frac{8}{9}\begin{pmatrix} N \\ 1 \\ 0 \\ \vdots \\ 0 \end{pmatrix} \widetilde{P}\,, \tag{C.12}$$

where

$$\begin{aligned} P &= (0, 0, -1/N, 1, -1/N, 1, 0), \\ \widetilde{P} &= (0, 0, 0, 0, 0, 0, 1). \end{aligned} \tag{C.13}$$

In summary, we find

$$\left[\widetilde{Q}_1^{(u)}\right]_1 \;=\; \frac{8}{3}\,(1-N^2)\,, \qquad \left[\widetilde{Q}_2^{(u)}\right]_1 \;=\; \frac{280}{81}\,(\frac{1}{N}-N)\,. \tag{C.14}$$

Step 3:
The contribution of $[\widetilde{Q}_1^{(d)}]_1$ to the seventh column can be related to the corresponding contribution of $[\widetilde{Q}_1^{(u)}]_1$ found in step 2. Inspecting the diagrams of fig. 4 we obtain

$$[\widetilde{Q}_1^{(d)}]_1 \;=\; -\,\frac{1}{2}\,[\widetilde{Q}_1^{(u)}]_1 \;=\; \frac{4}{3}\,(N^2-1)\,. \tag{C.15}$$

Step 4:
The calculation of $[\widetilde{Q}_2^{(d)}]_1$ proceeds as follows. Since $\widetilde{Q}_2^{(d)}$ receives contributions from both type-1 and type-2 insertions we can write

$$[\widetilde{Q}_2^{(d)}]_1 \;=\; [\widetilde{Q}_2^{(d)}]_{\rm p} - [\widetilde{Q}_2^{(d)}]_2\,, \tag{C.16}$$

with the last entry calculated in step 1.

In order to find $[\widetilde{Q}_2^{(d)}]_{\rm p}$ we compare the two–loop anomalous dimension matrices calculated in the bases D and B using the relation

$$(\hat{\gamma}^{(1)})_p^{(D)} \;=\; (\hat{\gamma}^{(1)})_p^{(B)} + \Big[(\Delta\hat{r})^{(d)}, (\hat{\gamma}^{(0)})^{(d)}\Big] + 2\,\beta_0\,\Delta\hat{r}^{(d)}\,, \tag{C.17}$$

where the index d indicates that now the auxiliary bases D and B are considered. The matrix $(\hat{\gamma}^{(0)})^{(d)}$ differs from $(\hat{\gamma}^{(0)})$ only in the first row and the entry $(2,7)$. The first row in $(\hat{\gamma}^{(0)})^{(d)}$ equals the second row and

$$(\gamma_{17}^{(0)})^{(d)} = (\gamma_{27}^{(0)})^{(d)} = \frac{8}{9}\,(N+1)\,. \tag{C.18}$$

$\hat{\gamma}^{(1)}$ and $(\Delta\hat{r})^{(d)}$ involve again only the penguin contributions. From one-loop penguin diagrams we find

$$(\Delta\hat{r})^{(d)} = \frac{1}{3}\begin{pmatrix} 1\\ -1\\ 0\\ \vdots\\ 0 \end{pmatrix} P - \frac{4}{9}\,(N-1)\begin{pmatrix} 1\\ -1\\ 0\\ \vdots\\ 0 \end{pmatrix}\widetilde{P}\,. \tag{C.19}$$

In this way the last two terms in eq. (C.17) can be evaluated. Since both types of insertions of $\widetilde{Q}_1^{(d)}$ have been calculated in steps 1 and 3, the element $\left[\widetilde{Q}_2^{(d)}\right]_1$ can finally be extracted from eq. (C.17) when in addition the relation (C.5) is used. The result is

$$\left[\widetilde{Q}_2^{(d)}\right]_1 \;=\; \frac{64}{81}\,(\frac{1}{N}-N)\,. \tag{C.20}$$

Putting all this together and using eqs. (C.6) and (C.7) we find the results for $\gamma_{37}^{(1)}$ and $\gamma_{47}^{(1)}$ for the NDR scheme quoted in eqs. (3.6) and (3.7), respectively.

D Collection of Numerical Input Parameters

Quark Masses

$$m_t = 120 \; - \; 250\,\mathrm{GeV} \qquad m_b = 4.8\,\mathrm{GeV} \qquad m_c = 1.4\,\mathrm{GeV}$$

QCD and Electroweak Parameters

$$\begin{array}{rclrcl}
\Lambda_{\overline{\mathrm{MS}}} & = & 200\,\mathrm{MeV}: & \alpha_s(M_Z) & = & 0.109 \\
\Lambda_{\overline{\mathrm{MS}}} & = & 300\,\mathrm{MeV}: & \alpha_s(M_Z) & = & 0.116 \\
\Lambda_{\overline{\mathrm{MS}}} & = & 400\,\mathrm{MeV}: & \alpha_s(M_Z) & = & 0.122 \\
\alpha & = & 1/128 & G_F & = & 1.16639 \cdot 10^{-5}\,\mathrm{GeV}^{-2} \\
\sin^2\theta_W & = & 0.23 & M_W & = & 80.0\,\mathrm{GeV}
\end{array}$$

CKM Elements and B_K Ranges

$$\begin{array}{lllll}
 & |V_{us}| = 0.22 & & & \\
\text{Range (a)}: & |V_{cb}| = 0.040 \pm 0.005 & |V_{ub}/V_{cb}| = 0.08 \pm 0.02 & B_{\mathrm{K}} = 0.70 \pm 0.20 \\
\text{Range (b)}: & |V_{cb}| = 0.040 \pm 0.002 & |V_{ub}/V_{cb}| = 0.08 \pm 0.01 & B_{\mathrm{K}} = 0.75 \pm 0.05 \\
\text{Range (c)}: & |V_{cb}| = 0.043 \pm 0.002 & |V_{ub}/V_{cb}| = 0.09 \pm 0.01 & B_{\mathrm{K}} = 0.55 \pm 0.05
\end{array}$$

K Decays and $K^0 - \bar{K}^0$ Mixing

$$\begin{array}{lrclrcl}
BR(K^+ \to \pi^0 e^+ \nu) = 0.0482 & m_{\mathrm{K}} & = & 498\,\mathrm{MeV} & \eta_1 & = & 1.1 \\
\tau_{K_L} = 5.17 \cdot 10^{-8}\,s & F_{\mathrm{K}} & = & 161\,\mathrm{MeV} & \eta_2 & = & 0.57 \\
\tau_{K^+} = 1.237 \cdot 10^{-8}\,s & \Delta M_{\mathrm{K}} & = & 3.5 \cdot 10^{-15}\,\mathrm{GeV} & \eta_3 & = & 0.36 \\
\epsilon = 2.258 \cdot 10^{-3} & & & & & &
\end{array}$$

$B^0 - \bar{B}^0$ Mixing

$$x_d \;=\; 0.72 \pm 0.08 \qquad \sqrt{B_B}\, F_B \;=\; 200 \pm 30\,\mathrm{MeV} \qquad \eta_{2B} \;=\; 0.55$$

E Tables

Table 1: Wilson coefficients at $\mu = 1\,\text{GeV}$ for $m_\text{t} = 150\,\text{GeV}$. In our approach $y_1 = y_2 \equiv 0$ holds.

	$\Lambda_{\overline{\text{MS}}} = 0.2\,\text{GeV}$			$\Lambda_{\overline{\text{MS}}} = 0.3\,\text{GeV}$			$\Lambda_{\overline{\text{MS}}} = 0.4\,\text{GeV}$		
Scheme	LO	NDR	HV	LO	NDR	HV	LO	NDR	HV
z_1	-0.583	-0.394	-0.474	-0.710	-0.483	-0.602	-0.848	-0.584	-0.769
z_2	1.310	1.196	1.248	1.398	1.254	1.337	1.500	1.325	1.462
z_3	0.004	0.008	0.004	0.005	0.013	0.008	0.007	0.021	0.015
z_4	-0.010	-0.023	-0.011	-0.013	-0.034	-0.018	-0.018	-0.054	-0.029
z_5	0.003	0.006	0.003	0.004	0.007	0.004	0.006	0.009	0.006
z_6	-0.010	-0.023	-0.010	-0.015	-0.035	-0.016	-0.020	-0.055	-0.026
z_{7V}/α	-0.015	-0.008	0.009	-0.026	-0.037	0.000	-0.037	-0.071	-0.009
y_3	0.027	0.022	0.024	0.033	0.028	0.032	0.041	0.035	0.042
y_4	-0.047	-0.043	-0.045	-0.055	-0.051	-0.054	-0.063	-0.059	-0.064
y_5	0.011	0.004	0.012	0.012	0.001	0.015	0.013	-0.008	0.018
y_6	-0.078	-0.071	-0.065	-0.101	-0.098	-0.086	-0.129	-0.141	-0.117
y_{7V}/α	0.554	0.718	0.711	0.524	0.708	0.700	0.498	0.698	0.688
y_{7A}/α	-0.579	-0.579	-0.579	-0.579	-0.579	-0.579	-0.579	-0.579	-0.579

Table 2: Wilson coefficient z_{7V}/α for $m_\text{t} = 150\,\text{GeV}$ for various values of μ.

	$\Lambda_{\overline{\text{MS}}} = 0.2\,\text{GeV}$			$\Lambda_{\overline{\text{MS}}} = 0.3\,\text{GeV}$			$\Lambda_{\overline{\text{MS}}} = 0.4\,\text{GeV}$		
μ[GeV]	LO	NDR	HV	LO	NDR	HV	LO	NDR	HV
0.8	-0.030	-0.020	0.010	-0.052	-0.067	-0.007	-0.075	-0.127	-0.021
0.9	-0.021	-0.013	0.010	-0.037	-0.049	-0.002	-0.053	-0.094	-0.015
1.0	-0.015	-0.008	0.009	-0.026	-0.037	0.000	-0.037	-0.071	-0.009
1.1	-0.009	-0.005	0.007	-0.017	-0.028	0.002	-0.025	-0.055	-0.005
1.2	-0.005	-0.004	0.005	-0.010	-0.023	0.002	-0.015	-0.044	-0.002

Table 3: Wilson coefficient y_{7V}/α for $m_{\rm t} = 150\,{\rm GeV}$ for various values of μ.

	$\Lambda_{\overline{\rm MS}} = 0.2\,{\rm GeV}$			$\Lambda_{\overline{\rm MS}} = 0.3\,{\rm GeV}$			$\Lambda_{\overline{\rm MS}} = 0.4\,{\rm GeV}$		
$\mu[\,{\rm GeV}]$	LO	NDR	HV	LO	NDR	HV	LO	NDR	HV
0.8	0.558	0.722	0.715	0.529	0.712	0.704	0.503	0.700	0.691
0.9	0.556	0.720	0.713	0.526	0.710	0.702	0.500	0.700	0.690
1.0	0.554	0.718	0.711	0.524	0.708	0.700	0.498	0.698	0.688
1.1	0.552	0.717	0.709	0.523	0.706	0.698	0.496	0.696	0.686
1.2	0.551	0.715	0.708	0.521	0.705	0.696	0.494	0.694	0.684

Table 4: Wilson coefficients y_{7V}/α (at $\mu = 1\,{\rm GeV}$) and y_{7A}/α for various values of $m_{\rm t}$.

	y_{7V}/α							y_{7A}/α
		$\Lambda_{\overline{\rm MS}} = 0.2\,{\rm GeV}$		$\Lambda_{\overline{\rm MS}} = 0.3\,{\rm GeV}$		$\Lambda_{\overline{\rm MS}} = 0.4\,{\rm GeV}$		
$m_{\rm t}[\,{\rm GeV}]$	No QCD	LO	NDR	LO	NDR	LO	NDR	
130	0.763	0.522	0.686	0.493	0.676	0.466	0.666	-0.464
150	0.795	0.554	0.718	0.524	0.708	0.498	0.698	-0.579
170	0.823	0.583	0.747	0.553	0.737	0.527	0.727	-0.703
190	0.849	0.609	0.774	0.580	0.763	0.553	0.753	-0.836
210	0.874	0.634	0.799	0.605	0.788	0.578	0.778	-0.978
230	0.898	0.658	0.823	0.629	0.812	0.602	0.802	-1.129
250	0.921	0.681	0.846	0.652	0.836	0.626	0.825	-1.290

Table 5: PBE coefficient P_0 of y_{7V} for various values of $\Lambda_{\overline{\rm MS}}$ and μ. In the absence of QCD $P_0 = 8/9\ \sin^2\theta_W \ln(M_W/m_c) = 0.827$ holds universally.

		P_0		
$\Lambda_{\overline{\rm MS}}[\,{\rm GeV}]$	$\mu[\,{\rm GeV}]$	LO	NDR	HV
0.2	0.8	0.487	0.725	0.714
	1.0	0.482	0.719	0.709
	1.2	0.477	0.715	0.704
0.3	0.8	0.446	0.711	0.699
	1.0	0.440	0.705	0.693
	1.2	0.434	0.700	0.687
0.4	0.8	0.408	0.694	0.681
	1.0	0.401	0.690	0.676
	1.2	0.396	0.684	0.670

Table 6: $BR(K_{\rm L} \to \pi^0\, e^+\, e^-)_{\rm dir} \cdot 10^{12}$ at $\mu = 1.0$ for $V_{cb} = 0.041$, $V_{ub}/V_{cb} = 0.10$, $B_K = 0.7$ and various values of $\Lambda_{\overline{\rm MS}}$ and $m_{\rm t}$. The labels (I) and (II) denote the two different solutions for the CKM phase δ.

		LO		NDR		HV	
$\Lambda_{\overline{\rm MS}}[\,{\rm GeV}]$	$m_{\rm t}[\,{\rm GeV}]$	(I)	(II)	(I)	(II)	(I)	(II)
	140	4.01	2.95	5.48	4.02	5.40	3.97
	160	4.70	2.44	6.08	3.15	6.01	3.11
0.2	180	5.18	2.20	6.41	2.72	6.35	2.70
	200	5.61	2.07	6.69	2.46	6.63	2.44
	220	6.02	1.98	6.96	2.29	6.91	2.28
	240	6.41	1.93	7.24	2.18	7.20	2.17
	140	3.79	2.79	5.38	3.95	5.29	3.89
	160	4.49	2.33	5.98	3.10	5.91	3.06
0.3	180	5.00	2.12	6.32	2.69	6.25	2.66
	200	5.45	2.01	6.61	2.44	6.55	2.41
	220	5.87	1.93	6.90	2.27	6.84	2.26
	240	6.28	1.89	7.18	2.16	7.13	2.15
	140	3.61	2.65	5.27	3.87	5.18	3.81
	160	4.32	2.24	5.89	3.05	5.80	3.01
0.4	180	4.84	2.06	6.24	2.65	6.16	2.62
	200	5.30	1.95	6.54	2.41	6.47	2.38
	220	5.74	1.89	6.83	2.25	6.77	2.23
	240	6.17	1.86	7.12	2.15	7.07	2.13

F Feynman Diagrams

Figure 1: One-loop current-current and penguin diagrams in the full theory.

Figure 2: The three basic ways of inserting a given operator into a four-point function: (a) current-current-, (b) type-1 penguin-, (c) type-2 penguin-insertion. The 4-vertices "$\otimes$ $\otimes$" denote standard operator insertions.

Figure 3: One-loop current-current and penguin diagrams contributing to $\gamma^{(0)}$ in the effective theory. The unlabeled wavy lines denote either a gluon or a photon. The meaning of vertices is the same as in fig 2. Possible left-right or up-down reflected diagrams are not shown.

Figure 4: Two–loop penguin diagrams contributing to $\gamma_{i7}^{(1)}$, $i = 1, \ldots, 6$. Square vertices stand for type-1 and type-2 penguin insertions as of figs. 2(b) and (c), respectively. Possible left-right reflected diagrams are not shown. The numbering of the diagrams corresponds to the notation in ref. [10].

G Figures

Figure 5: Wilson coefficients $|y_{7V}/\alpha|^2$ and $|y_{7A}/\alpha|^2$ as a function of m_t for $\Lambda_{\overline{\rm MS}} = 0.3\,{\rm GeV}$ at scale $\mu = 1.0\,{\rm GeV}1$.

Figure 6: Allowed ranges for $BR(K_L \longrightarrow \pi^0 e^+ e^-)_{\rm dir}$ as a function of m_t for $\Lambda_{\overline{\rm MS}} = 0.3\,{\rm GeV}$ at scale $\mu = 1.0\,{\rm GeV}$. The labels (I) and (II) refer to the two possible solutions for the CKM phase δ. Parameters $|V_{cb}|$, $|V_{ub}/V_{cb}|$ and B_K were varied within present experimental limits as given in (5.12). The light and dark shaded areas correspond to the LO and NLO results, respectively. The solid line inside the dark shaded area describes the additional restriction from B^0–$\overline{B}^0$ mixing (see the text).

Figure 7: The same as in fig. 6, but for the parameter range given in (5.13).

Figure 8: The same as in fig. 6, but for the parameter range given in (5.14).

Figure 9: $BR(K_L \longrightarrow \pi^0 e^+ e^-)_{\rm dir}/({\rm Im}\lambda_t)^2$ as a function of m_t for various values of $\Lambda_{\overline{\rm MS}}$ at scale $\mu = 1.0\,{\rm GeV}$.

References

[1] B. Winstein and L. Wolfenstein, *Rev. Mod. Phys.* **65** (1993) 1113.

[2] J. L. Ritchie and S. G. Wojcicki, *Rev. Mod. Phys.* **65** (1993) 1149.

[3] L. Littenberg and G. Valencia, *Ann. Rev. Nucl. Part. Phys.* **43** (1993) 729.

[4] M. Kobayshi and K. Maskawa, *Prog. Theor. Phys.* **49** (1973) 652.

[5] A. Wagner (NA31), *talk presented at the European Physics Symposium on High Energy Physics, Marseille, July 1993* .

[6] L. K. Gibbons *et al.*, *Phys. Rev. Lett.* **70** (1993) 1203.

[7] G. Altarelli, G. Curci, G. Martinelli, and S. Petrarca, *Nucl. Phys.* **B187** (1981) 461.

[8] A. J. Buras and P. H. Weisz, *Nucl. Phys.* **B333** (1990) 66.

[9] A. J. Buras, M. Jamin, M. E. Lautenbacher, and P. H. Weisz, *Nucl. Phys.* **B370** (1992) 69; addendum ibid. *Nucl. Phys.* **B375** (1992) 501.

[10] A. J. Buras, M. Jamin, M. E. Lautenbacher, and P. H. Weisz, *Nucl. Phys.* **B400** (1993) 37.

[11] A. J. Buras, M. Jamin, and M. E. Lautenbacher, *Nucl. Phys.* **B400** (1993) 75.

[12] A. J. Buras, M. Jamin, and M. E. Lautenbacher, *Nucl. Phys.* **B408** (1993) 209.

[13] M. Ciuchini, E. Franco, G. Martinelli, and L. Reina, *Phys. Lett.* **301B** (1993) 263.

[14] M. Ciuchini, E. Franco, G. Martinelli, and L. Reina, *Ecole Normale Superieure preprint* **LPTENS 93/11**.

[15] F. J. Gilman and M. B. Wise, *Phys. Rev.* **D20** (1979) 2392.

[16] F. J. Gilman and M. B. Wise, *Phys. Rev.* **D21** (1980) 3150.

[17] C. O. Dib, I. Dunietz, and F. J. Gilman, *Phys. Lett.* **218B** (1989) 487.

[18] C. O. Dib, I. Dunietz, and F. J. Gilman, *Phys. Rev.* **D39** (1989) 2639.

[19] J. M. Flynn and L. Randall, *Nucl. Phys.* **B326** (1989) 31.

[20] A. G. Cohen, G. Ecker, and A. Pich, *Phys. Lett.* **304B** (1993) 347.

[21] A. Pich, *CERN preprint* **CERN-Th-7114-93;** Bulletin Board: **hep-ph 9312297**.

[22] M. Misiak and Z. Płuciennik, *Phys. Lett.* **268B** (1913) 429.

[23] G. Buchalla, A. J. Buras, and M. K. Harlander, *Nucl. Phys.* **B349** (1991) 1.

[24] M. K. Gaillard and B. W. Lee, *Phys. Rev. Lett.* **33B** (1974) 108.

[25] G. Altarelli and L. Maiani, *Phys. Lett.* **52B** (1974) 351.

[26] M. A. Shifman, A. I. Vainshtein, and V. I. Zakharov, *JEPT* **45** (1977) 670.

[27] B. Guberina and R. D. Pecchei, *Nucl. Phys.* **B163** (1980) 289.

[28] J. O. Eeg and I. Picek, *Phys. Lett.* **214B** (1988) 651.

[29] M. Misiak, *Nucl. Phys.* **B393** (1993) 23.

[30] G. Buchalla and A. J. Buras, *Nucl. Phys.* **B398** (1993) 285.

[31] G. Buchalla and A. J. Buras, *Nucl. Phys.* **B400** (1993) 225.

[32] G. Buchalla and A. J. Buras, *Nucl. Phys.* **B412** (1994) 106.

[33] S. Herrlich and U. Nierste, *Technical University Munich preprint* **TUM-T31-49/93;** Bulletin Board: **hep-ph 9310311**.

[34] A. J. Buras, M. Jamin, and P. H. Weisz, *Nucl. Phys.* **B347** (1990) 491.

[35] W. A. Kaufman, H. Steger, and Y. P. Yao, *Mod. Phys. Lett.* **A3** (1988) 1479.

[36] G. Buchalla, A. J. Buras, and M. K. Harlander, *Nucl. Phys.* **B337** (1990) 313.

[37] A. Datta, J. Fröhlich, and E. A. Paschos, *Zeitschr. f. Physik* **C46** (1990) 63.

[38] J. M. Flynn, *Mod. Phys. Lett.* **A5** (1990) 877.

[39] G. W. Kilcup, S. R. Sharpe, and R. Gupta, *University of Washington preprint* **UW/PT-93-25**.

[40] W. Bardeen, A. J. Buras, and J.-M. Gérard, *Phys. Lett.* **211B** (1988) 343.

[41] J. Prades *et al.*, *Zeitschr. f. Physik* **C51** (1991) 287.

[42] A. S. Kronfeld and P. B. Mackkenzie, *Ann. Rev. Nucl. Part. Sci.* **43** (1993) 30.

[43] D. G. Cassel, *talk given at Max-Planck Institute, Munich, Dec. 15, 1993* .

[44] D. A. Harris *et al.*, *Phys. Rev. Lett.* **71** (1993) 3918.

[45] K. E. Ohl *et al.*, *Phys. Rev. Lett.* **64** (1990) 2755.

[46] G. Cella, G. Ricciardi, and A. Viceré, *Phys. Lett.* **258B** (1991) 212.

(a)
(b)
(c)
W
g,γ
g,γ,Z
(I)
(II)
0.0
2.0
4.0
6.0
8.0
10.0
12.0
120
140
160
180
200
220
240
m_t [GeV]
BR(K_L → π^0 e^+ e^-)_dir [10^-12]

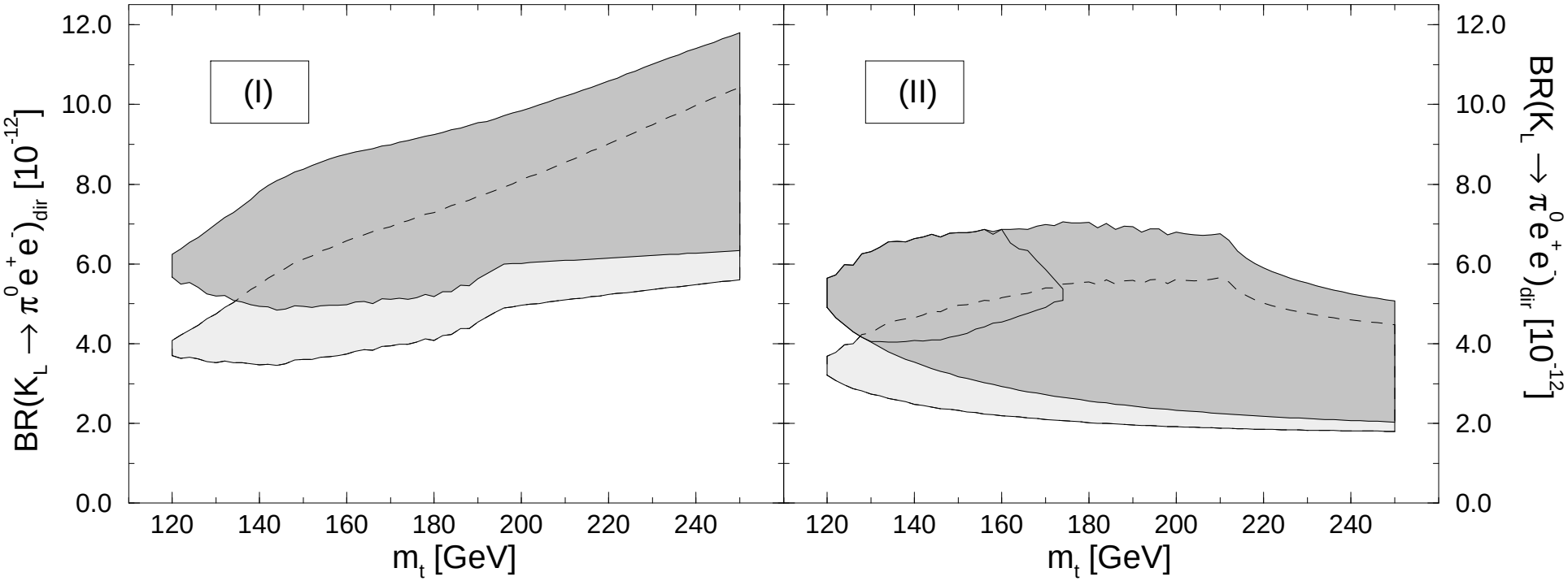
(I)
(II)
$BR(K_L \to \pi^0 e^+ e^-)_{dir}$ [10^{-12}]
m_t [GeV]
0.0
2.0
4.0
6.0
8.0
10.0
12.0
120
140
160
180
200
220
240

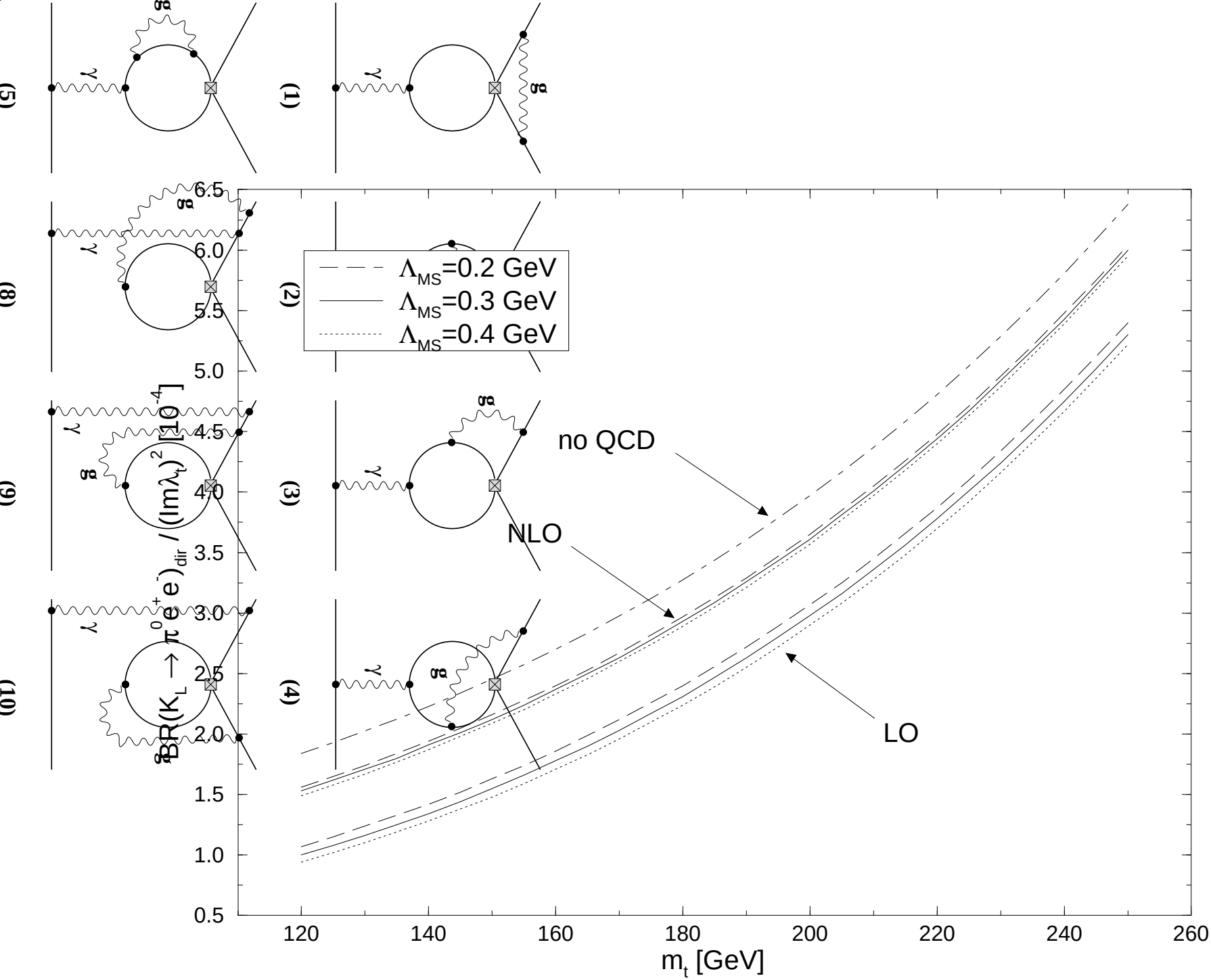
(1)
(2)
(3)
(4)
(5)
(6)
(8)
(10)
Λ_{MS}=0.2 GeV
Λ_{MS}=0.3 GeV
Λ_{MS}=0.4 GeV
no QCD
NLO
LO
$BR(K_L \to \pi^0 e^+ e^-)_{dir} / (\mathrm{Im}\lambda_t)^2$ [10^{-4}]
m_t [GeV]
0.5
1.0
1.5
2.0
2.5
3.0
3.5
4.0
4.5
5.0
5.5
6.0
6.5
120
140
160
180
200
220
240
260

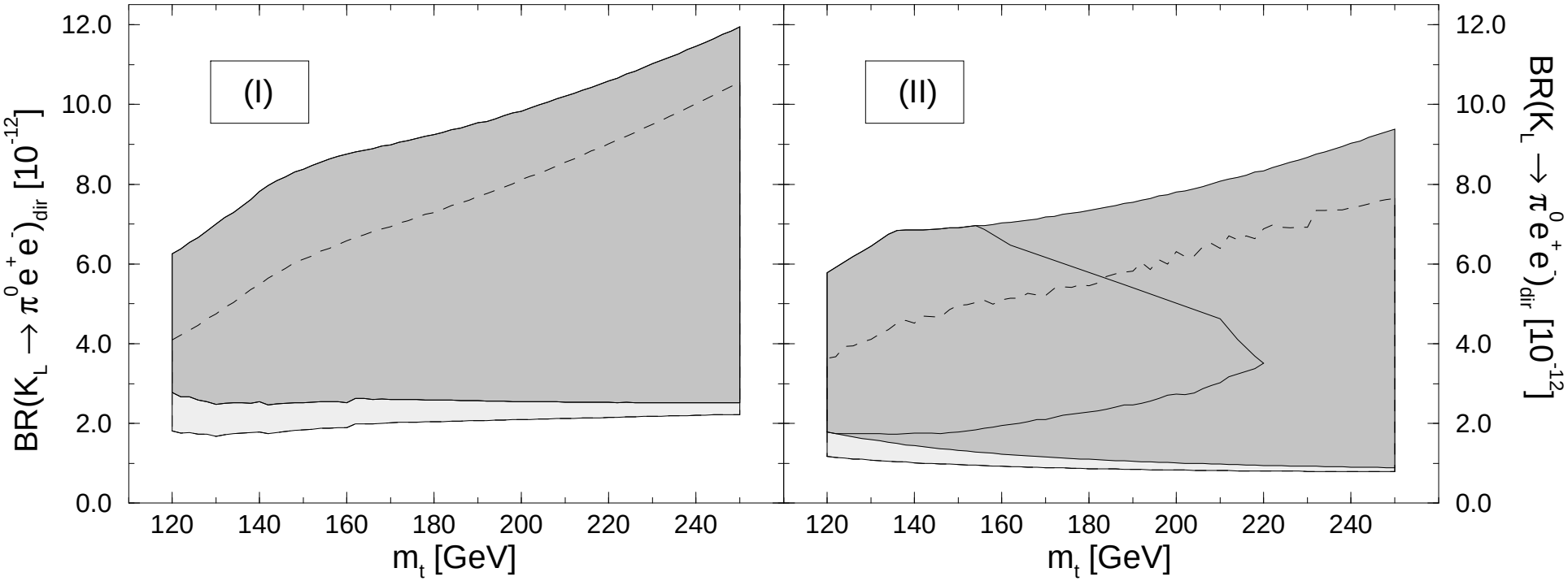
(I)
(II)
$BR(K_L \to \pi^0 e^+ e^-)_{dir}$ [10^{-12}]
m_t [GeV]
0.0
2.0
4.0
6.0
8.0
10.0
12.0
120
140
160
180
200
220
240

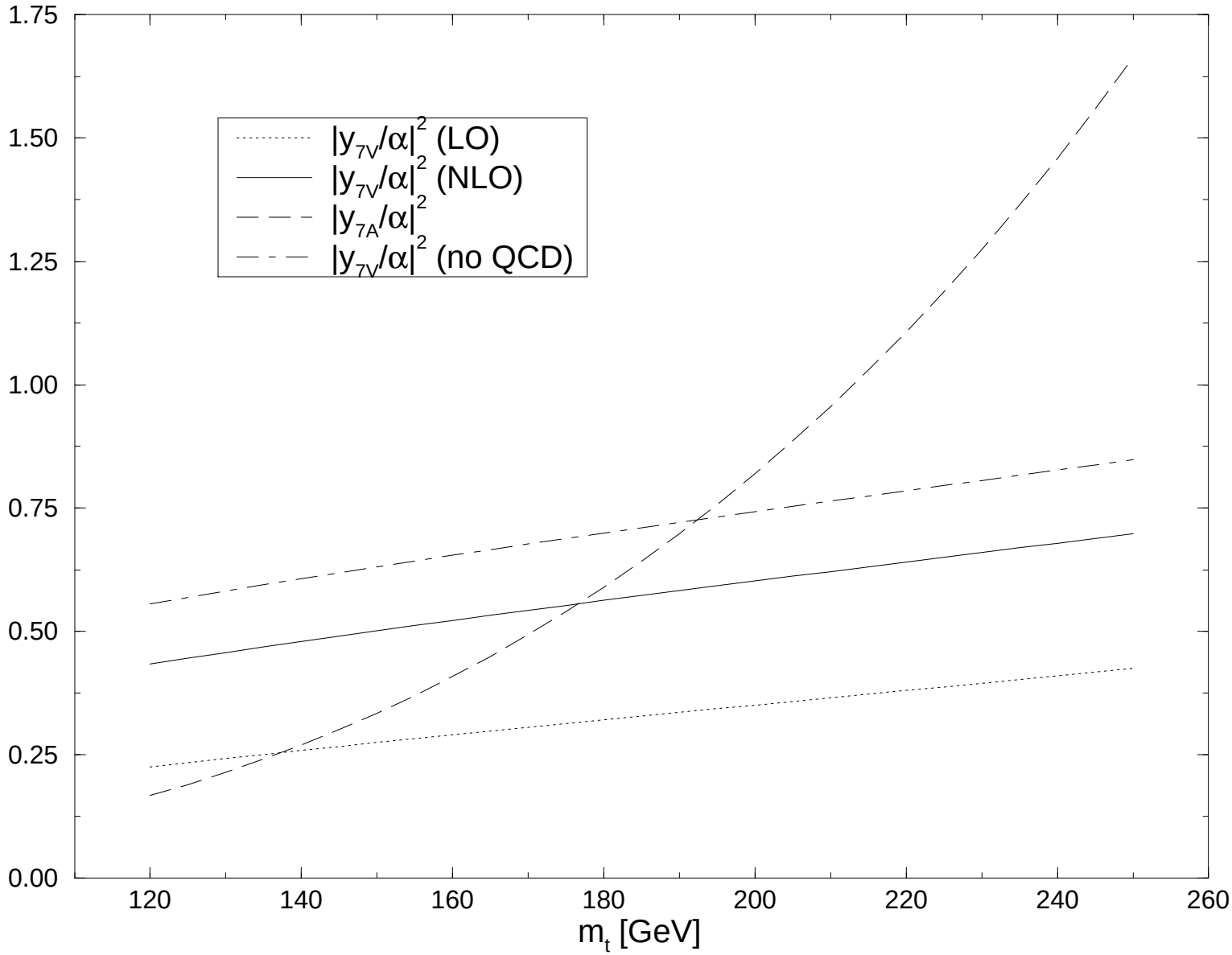
1.75
1.50
1.25
1.00
0.75
0.50
0.25
0.00
120
140
160
180
200
220
240
260
m_t [GeV]
$|y_{7V}/\alpha|^2$ (LO)
$|y_{7V}/\alpha|^2$ (NLO)
$|y_{7A}/\alpha|^2$
$|y_{7V}/\alpha|^2$ (no QCD)